Hydrogel nanoarchitectonics: an evolving paradigm for ultrasensitive biosensing

Zakia Sultana Nishat, Tanvir Hossain, Md. Nazmul Islam, Hoang-Phuong Phan, Md A. Wahab, Mohammad Ali Moni, Carlos Salomon, Mohammed A. Amin, Abu Ali Ibn Sina, Md Shahriar A. Hossain, Yusuf Valentino Kaneti,* Yusuke Yamauchi, Mostafa Kamal Masud*

Z. S. Nishat, T. Hossain, M. K. Masud
Department of Biochemistry and Molecular Biology, School of Life Sciences, Shahjalal University of Science & Technology, Sylhet 3114, Bangladesh.

T. Hossain, M. A. Wahab, Y. V. Kaneti, M. S. A. Hossain, Y. Yamauchi, M. K. Masud
Australian Institute for Bioengineering and Nanotechnology (AIBN), The University of Queensland, St. Lucia, QLD 4072 Australia.
Email: v.kaneti@uq.edu.au

M. N. Islam
School of Health and Life Sciences, Teesside University, Middlesbrough, Tees Valley, TS1 3BA, UK.

H.-P Phan
Queensland Micro and Nanotechnology Centre, Griffith University, Nathan, QLD 4111, Australia

M. A. Moni
School of Health and Rehabilitation Sciences, Faculty of Health and Behavioural Sciences, The University of Queensland, St Lucia, QLD 4072, Australia

M. A. Amin
Department of Chemistry, College of Science, Taif University, P.O. Box 11099, Taif, 21944, Saudi Arabia

C. Salomon
Exosome Biology Laboratory, UQ Centre for Clinical Research. Royal Brisbane and Women's Hospital, The University of Queensland, Herston, Brisbane City, QLD 4029, Australia

M. S. A. Hossain
School of Mechanical and Mining Engineering, Faculty of Engineering, Architecture and Information Technology (EAIT), The University of Queensland, Brisbane, QLD 40721, Australia.

Y. Yamauchi
School of Chemical Engineering, Faculty of Engineering, Architecture and Information Technology (EAIT), The University of Queensland, St. Lucia, QLD 4072, Australia.
Y. Yamauchi, M. K. Masud

JST-ERATO Yamauchi Materials Space-Tectonics Project and International Center for Materials Nanoarchitectonics (WPI-MANA), National Institute for Materials Science, Tsukuba, Ibaraki 305-0044, Japan.
Emails: masud.mostafakamal@nims.go.jp; m.masud@uq.edu.au

Keywords: hydrogel, nanoarchitectonics, biosensor, nanodiagnostics, nanobiotechnology

Abstract

The integration of nanoarchitectonics and hydrogel into conventional biosensing platforms offers the opportunities to design physically and chemically controlled and optimized soft structures with superior biocompatibility, better immobilization of biomolecules, and specific and sensitive biosensor design. The physical and chemical properties of three-dimensional (3D) hydrogel structures can be modified by integrating with nanostructures. Such modifications can enhance their responsiveness to mechanical, optical, thermal, magnetic, and electric stimuli, which in turn can enhance the practicality of biosensors in clinical settings. This review describes the synthesis and kinetics of gel networks and exploitation of nanostructures-integrated hydrogels in biosensing. With an emphasis on different integration strategies of hydrogel with nanostructures, this review highlights the importance of hydrogel nanostructures as one of the most favorable candidates for developing ultrasensitive biosensors. Moreover, we also portray hydrogel nanoarchitectonics as an auspicious candidate for fabricating next-generation robust biosensors.

1. Introduction

The demand for improved biosensing technologies for rapid diagnosis and monitoring of diseases has significantly increased in recent years to maintain a healthy lifestyle. Advanced biosensing technologies are critical in clinical care to fulfil the growing need for low-cost and rapid identification of disease-specific biomarkers, rigorous monitoring of health conditions, and tailored therapies. Biosensing utilizes specific bioreceptors (*e.g.*, enzyme, antibody, engineered aptamers, nucleic acids, *etc*.) to recognize the target biomolecules coupled with diverse transducing approaches to generate a quantifiable and detectable signal.[1–5] More specifically, the basic architecture of a biosensor consists of a receptor and a transducer. While the bioreceptor provides the selective site for identifying the target analyte for molecular recognition, the transducer transforms the recognition event of the target from the bioreceptor by transforming it into electrochemical, optical or other forms of a measurable signal. The key criteria for advanced biosensing technologies involve ultrasensitive detection, the requirement of small sample volume, low background noise and minimal chemistries for sensor surface functionalization and signal amplification. The advancement of nanotechnology allows these

criteria to be fulfilled by modifying the transducer with specially-designed nanoparticles (NPs) and nanostructures, such as gold (Au),[4,5] carbon nanotubes (CNTs),[6,7] graphene,[8] magnetic NPs (MNPs),[9,10] quantum dots (QDs).[11] These nanostructures-integrated biosensing are advantageous due to the quantum size effect, macro-quantum tunnelling, unique chemical and physical surface moiety, and controllable surface for biomolecule recognition.[10,12,13]

The emerging concept of "nanoarchitectonics" integrates conventional nanotechnology with supramolecular chemistry and biosciences to create novel functional nanostructures from nanoscale units.[13,14] Such combination enables the modulation of materials at atomic/molecular level and later translated their combined effect into nano/microscopic level. While not being the interchangeable term for pre-existing nanotechnology, nanoarchitectonics actually pushes the boundaries of conventional nanomaterial synthesis, modulation, and fabrication to a new horizon of material science. Apart from atomic/molecular-level manipulation, nanoarchitectonics also works by harmonizing uncontrollable factors, such as thermal fluctuation, statistical distribution, quantum effects. The nanoarchitectonics concept has been fueled by the saturation of nanotechnology and the subsequent inability to achieve advanced functions. Nanoarchitectonics has been applied in various biomedical applications, including tissue engineering, regenerative medicine, drug delivery, brain-like information processing, and biosensing. With the integration of nanotechnology, the biosensing field has already experienced improved functionality. However, some shortcomings still need to be addressed, such as the lack of understanding of sensing chemistry, low sensitivity, false positives and so on. This is because the structural motifs of sensors have largely been ignored and more focus has been put on developing novel sensing chemistry to improve the sensitivity of existing sensors. Thus, many biosensors still struggle to meet the end-user requirements. Hence, in order to improve the sensitivity and specificity of conventional biosensors, architecturing at the nanoscale is important and this can be achieved by atomic/molecular level manipulation, organic synthesis, self-assembly and self-organization and structural regulation. Despite the introduction of nanoarchitectonics and the related bottom-up fabrication procedures, there are still some challenges associated with biosensor construction, including poor biocompatibility, immunogenicity in real-time *in-vivo* screening, low

sensitivity and specificity arisen from the heterogenous nature of transduction surfaces, and complex bioreceptor functionalization chemistries involved in biosensor fabrication. These obstacles, particularly poor biocompatibility and low sensitivity can be addressed by utilizing hydrogels. Hydrogels are cross-linked 3D networks that entrap a large volume of fluid without being dissolved and undergo a rapid phase transition upon exposure to stimuli. The use of hydrogels in biosensors can provide improved biocompatibility, better biodegradability, exponentially scalable encoding capacities, suitable mechanical properties for nanostructures alignment, and 3D structured porous networks with the ability to retain a larger number of target biomolecules for ultrasensitive detection.[15,16] Furthermore, the salient properties of hydrogels, such as favorable rheology, biomimetic activity, ability to retain the native conformation of receptors, phase reversibility and excellent tailor-ability can provide high specificity. Conventional *in-vivo* biosensors may impart toxicity by generating reactive oxygen species (ROS), while hydrogel-based biosensors possess high biocompatibility. The integration of natural hydrogels with favorable geometries into diagnostic platforms can lower the fabrication cost. Hydrogel also serves as the foundational framework for different specialized structures including microrobots and actuators to stratify stimuli-responsive nanomaterials in a disk that may be adjusted for a variety of application scenarios.[17] Moreover, the facile incorporation of nanoarchitectonics into conducting polymers (CPs) can lead to higher conductivity, better sensing performance, and rapid signal transduction.

Briefly, hydrogel nanoarchitectonics promises biocompatibility as well as rapid and precise detection by regulating its incorporated nano-units and providing bioelectric interface fabrication coupled with self-assembly for both signal generation and transduction. Therefore, hydrogel nanoarchitectonics holds significant potential for manufacturing point-of-care (POC devices. The rapid responsiveness of hydrogels to external stimuli was first utilized in several biosensing platforms in the 1990s.[18–21] In 2004, a proof-of-concept for designing hydrogel biosensors was patented by Han and colleagues.[22] After that, rapid growth in biosensor research using hydrogels was observed for versatile analyte detection. With the gradual incorporation of two-dimensional (2D) nanostructures and zero-dimensional (0D) NPs, hydrogel-based biosensors have achieved robustness, specificity, and

meticulosity. Nanostructures-integrated hydrogels are mostly used as immobilizers of analytes, such as enzymes, probe molecules and antibodies,[23–25] as analyte respondents [26] and as conductive electrodes (**Scheme 1**).[27–29] Owing to their excellent mechanical properties, hydrogels are gaining increased popularity in the field of materials science. One of the most cited and comprehensive reviews on hydrogel preparation and characterization was provided by Enas M. Ahmed.[30] Several other useful reviews on the synthesis, properties and biomedical applications of hydrogels were also reported.[31–33] Various reviews on hydrogel-based biosensors have also been published.[34–37] These reviews described the synthesis and kinetics of gel network and focused mainly on pH-dependent biosensors. In contrast, our review focuses exclusively on the exploitation of hydrogels in biosensing rather than other biomedical applications.

Herein, we discuss the integration of hydrogels with nanoarchitectonics to achieve ultrasensitive detection by mentioning study-specific metrics which include detection limit, minimal range of detection. Moreover, we cover the physicochemical and thermodynamic properties of hydrogels and show how the inherent structural elasticity of hydrogels enables the incorporation of modified nano-units into hydrogels by nanoarchitectonics. Additionally, this review also covers the various bottom-up strategies for fabricating hydrogel-based biosensors. We anticipate that future research on biosensors will revolve around the integration of different NPs, nanocomposites and nanostructured film or electrodes with hydrogels to achieve highly sensitive and selective biosensors. Herein, we also portray integrated nanocomposite hydrogels as the most favorable candidates for developing state-of-the-art biosensors and reported the research evidence that convinced us to select hydrogels for fabricating highly robust next-generation biosensors.

2. Nanoarchitectured Hydrogel for Biosensing

Hydrogel is a 3D cross-linked polymeric network consisting of hydrophilic monomers that possess the essential inherent characteristics: bulk fluid retention, rapid phase transition (swollen/de-swollen), volume collapsed/de-collapsed, and dissolution resistance. The rational design of hydrogels depends on the target applications, for instance, hydrogels for drug delivery require high porosity, while

hydrogels for use in sanitary pads require high absorption capacity. Hydrogels are commonly prepared by the polymerization of hydrophilic monomers followed by the formation of crosslinking networks. The fabrication of hydrogels typically starts with the selection of the appropriate hydrophilic monomers, such as acrylic acid, methacrylic acid, acrylamide, 2-hydroxy methacrylate, hydroxyethyl methacrylate (HEMA), ethylene glycosyl dimethacrylate (EGDMA), vinyl acetate, N-isopropylacrylamide (NIPAAm), *etc*.[38,39] Polymerization techniques, such as bulk polymerization, photoinitiated polymerization, suspension or inverse- suspension, solution polymerization[30] have been used to form elastic polymeric networks. Crosslinking among polymers is required to avoid dissolution and this can be achieved in two ways- either through physical/reversible crosslinking (entanglements, Van der Waals interaction, electrostatic interaction, ionic interaction)[40,41] or by chemical crosslinking agents (such as ethylene glycol dimethacrylate, glutaraldehyde, N,N-(3-dimethylaminopropyl)–N–ethyl carbodiimide, epichlorohydrin), crosslinking condensation, high energy irradiation and so on.[42,43] The above general preparation method is clearly insufficient to certify hydrogel as a versatile applicant. That being the case, "fabrication" combined with cutting-edge imprinting techniques can enable the tailoring of hydrogels for the targeted application. Synthetic polymers (*e.g.*, polycaprolactone, poly (ethylene glycol) diacrylate (PEGDA), and polyvinyl alcohol (PVA)) can impart rheologically favorable behaviour which smoothens fabrication.[44] Layer-by-layer assembly, 3D printing, inkjet printing, fused deposition modelling, stereolithography, microfluidic fabrication strategies have been widely applied for preparing hydrogel nanostructures.[45–48] Nevertheless, all fabrication processes fail to maximize hydrogels' potential for biosensing purposes. Hence, it is important to sort out which tethering process is suitable for biosensing.

The emergence of nanoarchitectonics in the polymeric field results in the incorporation of nanomaterials into hydrogel networks. Such incorporation can impart advantages over conventional hydrogels, including high mechanical strength, enhanced conductivity, and tailorable shape. These attractive features can facilitate the fabrication of different biosensors and POC diagnostics. In recent years, nanoarchitectonics have been introduced into hydrogels to generate innovative superstructures for clinical diagnoses, such as magnetic guided drug targeting, hyperthermia treatment, magnetic

resonance imaging, and disease diagnosis.[49,50] Nanoarchitectonics bring diverse transformations of nano-units, such as 0D, 1D, 2D and 3D nano-units. By coupling equilibrium self-assembly and non-equilibrium self-organization processes, nanoarchitectonics can bring diversity to nanostructures. One of the important aspects of nanoarchitectonics is that it brings about various morphologies by controlling atomic arrangements through scanning probe microscopy (SPM), scanning tunnelling microscopy (STM). Being able to transform morphologies rather than just summing up units provide researchers with the maximum tools for modulating materials toward their favor. Nevertheless, this is challenging as some uncontrollable effects and uncertainties need to be resolved, while modulating structural motifs, such as thermal fluctuation, statistical distribution, quantum effect, undesirable agglomeration. To mitigate these challenges, it is important to develop and optimize techniques to harmonize these atomic/molecular-level effects without affecting the nano-/microscopic properties. Researchers have attempted to mitigate agglomeration by fabricating cage-ball nanoarchitectonics which may be useful to prevent internal agglomeration in hydrogel biosensors. Hierarchical functional materials hold great promise in multiplex biosensor fabrication. The inability to control the interfaces between the different layers of biosensors has been one of the stubborn problems in biosensor construction but interfacial nanoarchitectonics provides a way to address this by controlling surface design. Interfacial nanoarchitectonics directly bridges nanoscopic action and macroscopic function. Nanotechnology gives rise to many different nanostructures. It is important to achieve nanoarchitecturing of the sensing materials at the nanoscale to enhance the overall functionality of biosensors. One of the main advantages of nanoarchitectonics is it allows the plausible integration of diverse nano-units and this provides diversity in the design of biosensors. In this section, we have summarized different strategies for integrating nanostructures with hydrogels and discussed along with the pros and cons of each strategy. The potential routes for addressing the bottlenecks of biosensor construction by advancing nanoarchitectonics will be discussed as well.

2.1. Carbon-based Hydrogels

The integration of nanostructures into hydrogels can synergize efficacy as hydrogels alone possess low mechanical strength, while carbon nanostructures, such as graphene or CNTs are limited by low biocompatibility and cytotoxicity. By optimizing the synthetic procedures, the fusion of both carbon nanostructures and hydrogel can enable fine-tuning of the biosensing performance.[51] So far, carbon-based nanomaterials, such as graphene, CNTs, QDs have been successfully used in biosensors. The integration of hydrogels with graphene or its oxygenated derivatives (*i.e.*, graphene oxide (GO) and reduced graphene oxide (rGO))[52,53] make them less fragile. Porous CNTs with other polymeric compositions can enhance the porosity of hydrogels for rapid and stable bioreceptor encapsulation. With the introduction of engineered fabrication techniques, they offer conducive features and interfacial attributes which speed up signal transduction. The integration of carbon nanomaterials into the hydrogel network provides enhanced conductivity and chemical stability which are paramount for electrocatalytic and electrochemical biosensing.

Graphene-based hydrogels. Graphene is an allotrope of carbon (graphite) where a single layer of graphite sheet made of sp^2 hybridized carbon is arranged in a 2D crystalline structure. Graphene possesses attractive features for biosensing, such as superior conductivity, high thermal sensitivity and optical transparency.[54,55] Owing to these excellent characteristics, graphene is gradually replacing all other conventional nanomaterials in the biosensing field. Graphene incorporation can enhance the accuracy, specificity and sensitivity of conventional hydrogel biosensors. Further, the coupling of GO or rGO with natural polymers, allow it to be used in biosensors, bio-actuators, regenerative tissue fabricator, electrically conductive scaffolds/electrodes, analyte immobilization and drug delivery.[56–58] The conventional synthetic route for fabricating graphene hydrogels s is the self-assembly technique.[59] The gelation of GO,[60] the very first step of preparing graphene-based hydrogels, facilitates self-assembly. The self-assembly of graphene into a hydrogel typically is achieved using reduction methods, such as hydrothermal or solvothermal reduction, chemical reduction using reducing agents (ascorbic acid, $NaHSO_3$, Na_2S, HI)[61] and electrochemical reduction. Supramolecular interactions (*e.g.*, hydrogen bonding, π-π interactions, hydrophobic interaction, electrostatic interaction) play key roles in achieving tunable viscoelastic and rheological properties.[62] For

instance, Liu and colleagues utilized a hydrothermal method to synthesize rGO hydrogel for Biosensing.[63] They followed the hydrothermal one-step self- assembly method proposed by Xu and colleagues.[59] Zhu and colleagues reported composites of 3D graphene hydrogel (3DGH) and gold NPs (AuNPs) by using a one-step self-assembly process (**Figure 1a**).[64] They fabricated 3DGH-AuNPs on a glassy carbon electrode (GCE) for the simultaneous detection of ascorbic acid, dopamine and uric acid. Graphene oxide-polyacrylic acid (GO-PAA) nanocomposite hydrogel has also been prepared by Tai and colleagues.[65] Unlike the self-assembly method, they utilized an in-situ polymerization method, where GO was prepared by the Hummer method. GO/PVA nanocomposite hydrogel has been previously employed as a pH-sensitive biosensor, where PVA was used to promote physical crosslinking.[66] The chemical reduction of self-assembling graphene hydrogel has also been demonstrated.[67] In this method, sodium ascorbate was used as a reducing agent. A titanium oxide (TiO_2)-graphene nanocomposite hydrogel (TGH) has been prepared using a one-pot hydrothermal self-assembly process and utilized as an electrochemical biosensor.[68] Graphene hydrogel is also promising for fabricating advanced diagnostics for multiplex detection of bioanalytes. Recently, bioactive graphene hydrogels (as a gate material) were employed in field-effect transistor (FET) devices, where they were used to encapsulate biospecific receptors and preserve enzymes (**Figure 1b-c**).[69] To achieve selective patterning of polyethylene glycol (PEG) on top of individual graphene FET devices, spatially controlled photopolymerization was used. In comparison to a hydrogel-free enzyme (signal loss in 1 day), the graphene hydrogels could conserve the enzymatic activity over 1 week. This multiplexed FET device enabled the simultaneous detection of both penicillinase and acetylcholinesterase. The GO or rGO sheets can enable the encapsulation of metal nanostructures inside them through chemical reactions, *e.g.*, electrostatic interactions, covalent linkage and π-π stacking to generate a new class of hybrid materials for electrochemical biosensing and photothermal therapy, however, their long-term cytotoxicity should be considered when storing pre-fabricated sensor for long-term use.[70]

Carbon nanotube-based hydrogels. CNTs are another allotrope of carbon distinguished from graphene because of their structural arrangement, where sp^2 hybridized carbon atoms form hexagonal

lattices rolled up into cylindrical shapes.[71] Two types of CNTs have been discovered, namely single-walled CNTs (SWCNTs)[72] and multi-walled CNTs (MWCNTs). SWCNTs are defined as rolled-up graphene sheets made of honeycomb carbon lattice, arranged into three different shapes armchair, zigzag and chiral.[73] MWCNTs are concentric cylinders of stockpiled graphene sheets with a regular period of interspacing restricted under 15 nm. Chemical vapor deposition (CVD),[74] laser ablation,[75] electric arc- discharge[76] and gas-phase catalytic process (HiPco method)[77] are the conventional CNT production methods. The inherently high elasticity (Young's modulus = 1.25 TPa),[78] molecular stiffness, and high tensile strength of CNTs (resulting from its helicity) can lead to high ductility. Moreover, the electronic density, optical absorption, electron transfer properties of CNTs favors the fabrication of filed-effect transistor facilitating conducive sensing.[79,80] However, the high cytotoxicity,[81,82] hydrophobicity, resistance on interfacing with biomolecules, ROS generation, and agglomeration tendency of CNTs have limited their biomedical applications. To overcome these limitations, exohedral and endohedral functionalization of CNTs have been introduced by various means, yielding biocompatible, hydrophilic surfaces without affecting their good electrical conductivity and mechanical, and thermal properties. The hydrophobic surface of pristine CNTs has been modified through dispersion in organic solutions (*e.g.*, N, N-dimethylformamide (DMF), N-methyl pyrrolidinone) followed by ultrasonication. The functionalization of CNTs has been achieved by adding polar moiety onto the CNT surface either *via* covalent or non-covalent side wall attachment.[83–87] The facile method to solubilize CNTs is to wrap its surface with polymers, such as polyvinylpyrrolidone (PVP), polystyrene sulfonate (PSS), polyvinyl sulphate, and PEG.[88] The control of CNTs over biological systems can be achieved through these superficial modifications, which makes CNT-based hydrogels highly promising for constructing robust biosensors. CNTs can be employed as reinforcing agents in hydrogel networks, as well as making the hydrogel responsive to external electrical or thermal stimuli.[89]

The fabrication of CNT-based hydrogels typically involves the dispersion of pristine or functionalized CNTs in solution followed by incorporation into the hydrogel system by sonication. Optical and thermal-sensitive hydrogels were synthesized using N-isopropyl acrylamide as a

monomer, N, N′-methylene-bis-acrylamide as a photoinitiator for polymerization reaction, 2,2′-diethoxyacetophenone as a cross-linker and sodium deoxycholate as a surfactant for facilitating the infusion of CNTs into poly (N-isopropyl acrylamide) (PNIPAM).[90] The dispersion of SWCNTs has been achieved using ultrasonication. Through comparative swelling behavior and tensile tests, Tong and colleagues showed that CNT/PVA hybrid hydrogel exhibited better swelling and higher mechanical strength than conventional PVA hydrogel.[91] To achieve better dispersion, the CNTs were soaked into a HNO_3/H_2SO_4 (1:3, *v*/*v*) mixture solution before mixing with PVA. Additional carboxyl, carbonyl and phenol groups were also added to ensure homogeneous dispersion. They utilized the freezing/thaw cycle for the synthesis of CNT/PVA hydrogel system. Tungkavet and colleagues have reported the synthesis of MWCNT/gelatin hydrogel with a high aspect ratio,[92] in which the high entanglement and bundling favored high mechanical strength to overcome the shortcomings of non-composite hydrogel in biosensing applications. As one of the primary concerns of utilizing hydrogels in biosensing is the ability to respond rapidly to stimuli, several sensitive/responsive CNT composite hydrogel systems have also been reported in recent literature. Temperature-responsive N-isopropyl acrylamide hydrogel system was previously fused with MWCNTs where tetra-ethylene glycol dimethacrylate (TEGDMA) was used as a crosslinker, ethanol used as a solvent for polymerization and surfactants used to ensure complete dissolution and uniformity.[93] Poly (N,N-diethylacrylamide) (PDEA) hydrogel system is well known for being thermoresponsive. By infusing it with functionalized MWCNTs, poly (N,N-diethylacrylamide-co-acrylic acid)-functionalized MWCNTs were achieved as validated and characterized by Raman spectroscopy and Fourier transform infrared (FTIR) spectroscopy.[94] Using a semi-interpenetrating network (semi-IPN), Liu and colleagues utilized polyaniline (PAni) hydrogel to enhance the swelling properties of the resulting poly(acrylamide-co-sodium methacrylate)/PAni/carboxyl-functionalized MWCNTs.[95] Lee and colleagues utilized click chemistry (azide alkyne cycloaddition) onto SWCNTs with alkyne functionalized PVA to merge the two systems.[96] They used dimethysulfoxide (DMSO) to disperse SWCNTs with a-PVA. The gelation or crosslinking process was achieved *via* a Cu-catalyzed click reaction followed by electropolymerization.

2.2. Conductive Polymer Hydrogels

Polymeric hydrogel serves a different purposes in hydrogel nanotechnology for various applications including biosensing and biomimetic activity. They are widely used to avoid the degradation and excretion of nanostructured material during synthesis. Moreover, they can be tuned to similar sizes and shape human cells and biomolecules. For instance, PEG hydrogel can be engineered to human red blood cells (RBCs) with homologous size and higher elasticity 130-fold lower modulus than human RBCs).[97] Polymers that possess intrinsic conductivity have been used extensively in electrochemical sensors as their conductive nature is essential for biosensing purposes. Doping engineering has enabled the successful incorporation of conductive polymers, such as poly (3,4-ethylene dioxythiophene) (PEDOT), polythiophene (PTh), polypyrrole (PPy), PAni into hydrogels to obtain conductive polymer hydrogels (CPHs) that bridge between biology and electronics. In such composites, both organic conducting polymers (CPs) and hydrogels synergize each other by suppressing the immunogenicity and cytotoxicity of conductive polymers and reducing the brittleness and fragility of hydrogels. CPHs provide macroporosity, high surface matrices for the encapsulation of biorecognition molecules/species, adjustable mechanical strength, rapid recovery from bending, twisting and stretching, rapid electron transfer, a biocompatible interface between electrode and electrolyte, tuneable surface morphology, and facile micropatterned lithography for low-cost fabrication as well as accurate and rapid detection.[98,99] The fundamental synthetic route for CPHs mostly revolves around template guided method, surface matrix, network penetration, and introduction of dopant ions to activate the charge transfer pathway. Green *et al.* demonstrated the successful deposition of CPHs and CPs within hydrogel matrix.[100] Martin proposed a template-based method to synthesize CP-coated electrochemical film where they coated the metal film onto the surface of nanoporous polycarbonate filtration membrane.[101] Dopant-enabled supramolecular approach was used to synthesize CPH, where CuPcTs (copper phthalocyanine-3,4′,4′′,4′′′-tetrasulfonic acid tetrasodium salt) was utilized as both crosslinker and dopant for the PPy hydrogel.[102] Hydrogel-encapsulated electrodes were prepared using hydrogel as the supporting

matrix and PPy as the CP.[103] Pan and colleagues fabricated an amperometric glucose biosensor based on PAni/GO hydrogel using an ink-jet method (**Figure 2a-b**).[104] They used phytic acid as a gelating agent and dopant to form a CP (conductivity ≈ 0.11 S cm^{-1}). Phytic acid reacted with PAni to form a mesh-like hydrogel network and the polymerization process was achieved using an oxidative initiator. Thermogravimetric analysis (TGA) revealed that this composite hydrogel contained 93% water. The capacitance of the as-prepared electrode was ≈ 480 F g^{-1} with a fast response time of ~0.3s, and a sensitivity of ~16.7 μA mM^{-1} for glucose detection. Chitosan has also been integrated with CNT for obtaining conductive CNT hydrogel (**Figure 2c-e**). This hydrogel exhibited promising activity against a bioelectrochemical system (BES).

PPy hydrogel/Au composite was synthesized to fabricate an immunosensor for detecting carcinoembryonic antigen (CEA).[105] In this design, pyrrole was used as a monomer, phytic acid was employed as both dopant and gelating agent, ammonium persulfate was used as an initiator of the PPy network. For fabricating the immunosensor, AuNPs were electrodeposited onto glassy carbon electrodes. The conductivity of this electrode was ≈ 0.46 S cm^{-1} and the water content of this hydrogel was ≈ 94.5% (*w/w*) and the surface area of the hydrogel was 26.2 m^2 g^{-1}. A similar interpenetration method was used to fabricate PPy/PNIPAM and PAni/PNIPAM CPHs with electrical conductivity of 0.8 S m^{-1} and 11 S m^{-1}, respectively.[106] Inkjet-printed amperometric multiplexed biosensors were fabricated using PANI hydrogel incorporated with Pt nanoparticles (PtNPs).[28] In this study, a mixed solution of lipase, glycerol kinase and L-α-glycerophosphate oxidase were printed on PAni hydrogel interfaced on polyethylene terephthalate (PET) film by a "drop on demand" strategy. Li and colleagues fabricated a nanostructured CPH biosensor with PAni/PtNPs modified GCE as the working electrode, phytic acid as crosslinking and doping agents, and aniline as the monomer. For generating PtNPs, they used formic acid to reduce chloroplatinic acid. The resulting CPH biosensor exhibited wide linear ranges of 0.07-1 mM for uric acid, 0.3-9 mM for cholesterol and 0.2-5 mM for triglycerides and rapid response time of around 3 s.[107]

Humpolicek and colleagues reported the development of a biocompatible and conductive PAni cryogel from the polymerization of PAni from aniline monomer with ammonium peroxydisulfate

which was frozen in solid carbon dioxide suspension in ethanol at – 78 °C.[108] The resulting PAni cryogel consisted of 2 wt.% PAni, 5 wt.% PVA, and 93 wt.% water. This cryogel showed no cytotoxicity and embryotoxicity, rendering it highly promising for *in-vivo* implantable biosensing. Apart from the above-mentioned strategies, electrodeposition has also been utilized to prepare conductive electrodes based on CNT hydrogels. A self-assembled CNT-hydrogel was fabricated using the simultaneous electrodeposition of both CNTs and chitosan onto a carbon paper electrode.[109] As shown in **Figure 2(c-e)**, under the potential of −3 V, the H^+ in the CNT colloidal solution was reduced to hydrogen and deposition occurred, while the local high pH on the electrode surface promoted a sol-gel transition of chitosan (pH-responsive). The generated H_2 bubbles serves as templates for the formation of porous CNT hydrogels on the carbon paper surface. This electrode showed superior performance in a bioelectrochemical system owing to the high conductivity of CNTs and the high content of oxygen-containing functional groups (C—OH, C═O, *etc*.) on the surface of CNTs. This strategy was straightforward, and it provided a potential route for the single-step fabrication of nanostructured-hydrogel on any conductive surface.

2.3. DNA-Based Hydrogels

In contrast to molecular biologist and geneticist who consider DNA as information repertoire and structural unit of heredity, polymer chemists or material scientists treat DNA just like another natural polymer which possesses the potential to beat other polymers due to having a feasible route that allow scientists to reorient its inherent complementarity (Watson Crick base pairing) and hybridization nature. The discovery of supersecondary structures of DNA (i-motif (cytosine rich quadruplex structure governed by Hoogsteen base pairing), G-quadruplex (guanine rich)) and gelation upon their hybridization ease its utilization to yield gel-like polymers. The competitive metal affinity of DNA gels (Y-shaped, three interlocked ssDNA made of palindromic repeat forming gels aided by Linker Adapt) attracts organometallic polymer chemists to exploit them for sensing.[110] In addition, the rapid transition from sol to gel, gel to sol and the favorable rheology of DNA hydrogel open avenues for its utilization in biosensors. Using DNA itself as cross linker, utilizing its super secondary motifs to form

the gel network and incorporating aptamer (short oligonucleotide sequence obtained by combinatorial biology method named SELEX; systemic evolution of ligands by exponential enrichment into the hydrogel network is the traditional synthetic route for preparing a DNA hydrogel.[111,112] Moreover, designed secondary DNA motifs, such as i-motif, antisense DNA, DNAzyme, can act as bioreceptors and are immobilized into the hydrogel matrix.

Interlocked DNA structures have been molecularly engineered and aided by LinkerAdap to self-assemble and form a hydrogel. Xing and colleagues designed a Y-shaped DNA made of three single strands with sticky ends.[113] The hybridization between the Y scaffold and LinkerAdap led to the formation of a hydrogel. Firstly, Y scaffold and Linker DNA were separately designed, and agarose gel electrophoresis was performed to confirm their formation. A stoichiometric mixture of Y scaffold and Linker eventually formed a gel-like appearance. The rheology test showed that the shear storage modulus (G') was higher than the shear loss modulus (G''), which validated the gel-like state. To confirm the responsiveness, they introduced the prepared hydrogel with enzyme and thermal change. Through enzymatic ligase -catalyzed reaction, the formation of DNA hydrogel from Branched DNA Molecule (BDM) was demonstrated by Um and co-workers.[114] Three BDMs of different shapes (X, Y and T, having complementary palindromic sequence on their sticky ends) were used to compare their tensile module and swollen/deswollen state. To form a hydrogel, the three BDMs were separately ligated by T4 DNA ligase. X-DNA gel was reported to have the highest tensile module. Their inner structures in both swollen and deswollen conditions were characterized by atomic force microscopy (AFM), field-emission scanning electron microscopy (FESEM) and confocal microscopy. Jiang and colleagues proposed a low-cost self-assembled one strand and two strands DNA hydrogels by using ssDNA which had a multidomain palindromic unit (**Figure 3a**).[115] Firstly, structurally- defined DNA motif with self-complementary palindromic unit was designed. To verify the length of the DNA motifs, they purified the designed DNA motifs by Polyacrylamide gel electrophoresis (PAGE) and to test mobility, they performed polyacrylamide gel run. The rheology tests confirmed their gel-like properties. Cheng *et al.* proposed a similar approach to create a pH-triggered responsive hydrogel where they used a Y-shaped DNA motif which eventually formed i-

motif (tetraplex domain) and mixed a stoichiometric amount of the DNA strand in a MES (2-(N-morpholino)ethanesulfonic acid) buffer. Here, the formation of the desired DNA was confirmed by polyacrylamide gel electrophoresis.[116] The rheology test showed that this system became hydrogel at a concentration of 0.5 mM. Photoresponsive DNA crosslinked hydrogel was prepared by crosslinking two ssDNA strands with Azo-incorporated DNA strand. Upon exposure to UV light, it changed from gel to sol state.[117] In this process, two DNA polyacrylamide conjugates (DPC-A and DPC-B) were synthesized by photoinitiated polymerization of acydite oligonucleotide monomer followed by their interlinking *via* the azo-incorporated DNA crosslinker consisting of 24 base DNA strands with 11 azo incorporations. Stoichiometric measurements of these three solutions at 3 mM concentration with further heating and cooling resulted in the formation of hydrogels. Ag^+-induced assembly of DNA hydrogel was proposed where Y strands crosslinked through a linker strand *via* the cytosine-Ag^+-cytosine bridge. Exposure to cysteamine attracted Ag^+ which disrupted the hydrogel network.[118] This principle can be exploited for the sensing of bioanalytes.

The pH triggered secondary i-motif structure has been utilized to develop DNA hydrogel biosensors. The main principle is based on the pH-dependent switching of i-motif formation/deformation and subsequently, the gel network assembly/disassembly.[119,120] Rolling circle amplification for this type of hydrogel formation was proposed.[112] Lu and colleagues proposed a K^+-induced hemin/G-quadruplex hydrogel system which was formed *via* cross-linkage among acrylamide copolymer chains (**Figure 3b**).[121] Their polymerization was carried out by mixing acrylamide monomer and acrydite-oligonucleotides yielding acrylamide:acrydite-oligonucleotide copolymer. Upon the presence of K^+ ion, they formed a G-quadruplex structure which crosslinked polymer chains and led to gelation. This hydrogel collapsed upon the introduction of 18-crown-6-ether. Moreover, the incorporation of hemin into this hydrogel led to a mimicking ability similar to horseradish peroxidase (HRP) which further improved the biosensing performance.

Exploiting the specificity of molecularly-engineered aptamers, responsive DNA hydrogel systems have been designed.[122] The basic scheme of this approach is to incorporate aptamer within the linker DNA where exposure to the target analyte disrupts the gel network. Liu and colleagues

designed an ATP aptamer to yield ATP-sensible hydrogel[123]. They first designed an ATP-specific aptamer and linked it within the linker DNA. The linker DNA further bonded to the Y scaffold to form a hydrogel network. Another stimuli-responsive DNA hydrogel was proposed using two Y-shaped monomers and linker DNA to form hydrogel and GSH (gamma-glutamyl-cysteinyl-glycine).[124] Lin *et al.* fabricated an aptamer-based chemiluminescent biosensor for the specific detection of adenosine.[125] They used acrydite adenosine aptamer, acrydite ssDNA, and hemin aptamer to produce the DNA hydrogel. They further modified this DNA hydrogel with a Cu-based metal-organic framework HKUST-1 incorporated with AuNPs (Au@HKUST) to obtain a peroxidase-like activity. In the presence of Hemin, (Au@HKUST) formed G-quadruplex followed by the presence of adenosine to generate a readout signal. Cai and co-workers reported an electrochemical impedance biosensor for Hg^{+} detection based on DNA hydrogel by coupling with DNAzyme-assisted target recycling and hybridization chain reaction.[126] They first synthesized two acrylamide DNA polymer chains and merged it with Mg^{+} DNAzyme, leading to the formation of a hydrogel. This solution was coated into the surface of a GCE electrode and hybridization occurred *via* a hybridization chain reaction (HCR). Through electrochemical impedance spectroscopy, the signal was measured. He and colleagues fabricated a ratiometric surface-enhanced Raman spectroscopy (SERS) biosensor for detecting mRNA.[127] In this assay, two DNA strands were polymerized with tetramethylethylenediamine followed by incorporation of glucose oxidase (GOx) and linker DNA. Additional synthesis steps were performed to utilize the Raman probe for signalling. Au nanoflakes (AuNFs) were incorporated into a silicon wafer (Si@AuNFs). Next, 3- mercaptophenylboronic acid (MPBA) was incorporated into Si@AuNFs to form Si@AuNF@3-MPBA conjugates which were further integrated with the prepared DNA hydrogel. The main role of DNA hydrogel was to retain the native conformation of GO as it played an important role in detecting mRNA-122. Mao *et al.* fabricated an electrochemical biosensor where they utilized a DNA hydrogel as a scaffold for electron transfer.[128] In this biosensor, self-assembled DNA hydrogel was intercalated with electron mediators and additional Hemin/G-quadruplex was functionalized on indium-tin oxide (ITO) electrode. The fabrication of DNA hydrogel on the ITO electrode was performed by hyperbranched rolling circle

mechanism (HRCM). Here, DNA polymerase was added to initiate the linear rolling circle mechanism (LRCM) andAntisense DNA was employed to form hydrogel matrix for the colorimetric detection of DNA.[129] They used acrydite DNA as a crosslinker to form the gel network, while DNA-functionalized AuNPs was used for the sensing. DNAzyme has become attractive for ultrasensitive detection as it can be easily assembled into a gel matrix, and it can mimic HRP facilitating naked-eye detection. One of the most used DNAzymes for naked eye peroxide detection is G-quadruplex/hemin system. Mao and co-workers reported the fabrication of DNAzyme-functionalized hydrogel for visible detection of tumor DNA.[130] This DNA-based biosensor could detect tumor DNA with concentrations ranging from 1 pM to 10 nM and the LOD reached down to 0.32 pM. Zhao and colleagues proposed the colorimetric detection of peroxide using DNAzyme.[131] T-4c 15s-T DNA was used to form G-quadruplex which was subsequently incubated with hemin to form DNAzyme. This DNAzyme was incorporated into the gel matrix to form DNAzyme-functionalized hydrogel.

3. The Underpinning Intrinsic Properties of Hydrogel that Govern Biosensing

Hydrogels are well-known as “smart materials” owing to their intrinsic stimuli-responsiveness. External stimuli, such as physical triggers (pH, temperature, shear-stress) and chemical triggers (redox potential, ionic potential) can lead to significant changes in hydrogels. In terms of biosensing, analyte-receptor chemistry induces these external stimuli, leading to massive changes in the network (volume collapse, swelling, color change, and phase transition) (**Figure 4**). These inherent signal generating properties of hydrogel explored by non-equilibrium continuum theory reveal that sequential stimuli bring about osmotic swelling and travelling color waves which would assist in achieving complex signalization from a comparatively general hydrogel system.[132] Sensitivity arises from the highly responsive, reversible nature and degree of elasticity of hydrogels governed by their intrinsic thermodynamics, gel kinetics and inherent rheology. Investigating these intrinsic properties is crucial to tailor the properties of hydrogels. While with the incorporation of nanoarchitectonics into hydrogels can lead to better biosensing performance, more innovation and sophistication in hydrogel-

based biosensor construction. The fundamental properties of hydrogel that are routinely exploited in biosensing are as follows;

Phase transition. The presence of analyte induces changes in the temperature of the gel network which lead to phase transition (gel to sol, sol to gel). Uncrosslinked (sol state) PNIPAM hydrogel can be crosslinked (gel state) by thermal induction.[133][134] Thermally-induced changes bring about an intermediate phase where the system tries to reach equilibrium and settle into another phase. Phase separation depends on the low critical solution temperature (LCST). If the system's temperature is above LCST, it remains in the gelation phase, otherwise, it becomes miscible and the system is no longer a gel. The LCST of a system is dependent on the equilibrium of the polymer-polymer and solvent-polymer interactions. Equilibrium swelling theory describes the sol-gel phase transition in terms of Gibbs free energy. Polymer-polymer interaction is denoted as $\Delta G_{\text{elasticity}}$ and polymer-solvent interaction is denoted ΔG_{mixing}. The gel state is pre-dominated by $\Delta G_{\text{elasticity}}$ and when ΔG_{mixing} increases as a result of thermal induction, the gel matrix starts to swell and unlinked. Gradually, ΔG_{mixing} surpasses $\Delta G_{\text{elasticity}}$ and instantaneously phase transition occurs.[37] Oppositely, the removal of thermal stimuli results in gelation where $\Delta G_{\text{elasticity}} > \Delta G_{\text{mixing}}$. Thus, the analyte-induced switchable sol-gel phase transition property of hydrogel is favorable for biosensing.

Phase transition affects the mechanical behaviour of the PNIPAM hydrogel.[135] The change in pH induces phase transition as well[136]. Extensive studies on the thermodynamics of phase transition of PNIPAM hydrogel revealed its coexistent phase that undergoes inhomogeneous deformation.[134] A multiphysical generalized model for liquid-solid phase transition of physical hydrogel revealed that crosslinking density is small in the solution phase but large in liquid phase, implying that phase transition is affected by the crosslinking density of the gel network.[137] Monitoring of the dynamic phase transition of thermosensitive hydrogel showed that upon photonic stimuli, the thermosensitive hydrogel transited between hydrophilic and hydrophobic phases, leading to changes in its refractive index and temperature which could be tailored for sensing purposes.[138] Stimuli-responsive tetra PEG hydrogel underwent a reversible sol-gel-sol phase transition by utilizing strong non-covalent interaction of biotin-avidin conjugates in the presence of an analyte.[139] Consideration of stimuli-

induced phase transition is one of the primary factors in selecting a polymer network to design responsive hydrogel.

Swelling behavior. Hydrogel swelling results from the transition of the polymer network from glassy state to a rubbery state induced by medium temperature. When the glass transition temperature (T_g) of the polymer is lower than the medium temperature, the polymer chains become highly mobile, allowing easy penetration of the solvent into the mesh network this is termed as the glassy state. Conversely, when the medium temperature reaches over T_g, the polymer mobility lessens and solvent penetration becomes restricted – this is referred to as the rubbery state. The rate of swelling is determined by the extent of porosity. The molecular diffusion mechanism usually contributes to the swelling of the polymeric network. According to the Flory-Rehner theory, the swelling kinetics of hydrogel is governed by the thermodynamic free energy of mixing and elasticity of the gel-solvent system. In the swelling process, swelling favors force increase, while swelling restricts force. When both forces become equal, the system reaches equilibrium and no more additional swelling occurs. The swelling of the matrix results in enlarged mesh size (physical distance between polymer chains where solute can diffuse). Subsequently, immobilized receptors and colorimetric agents are released from the network if the network is irreversible or overcomes elasticity. In absence of stimuli, the hydrogel remains in a glassy state, and upon stimuli, it becomes swollen but before that, an intermediate glassy-rubbery state occurs. Rapid swelling rate is one of the determining factors for achieving highly sensitive biosensors. Bennour and colleagues synthesized poly N-dimethylacrylamide-co-maleic acid and their characterization showed that its swelling behaviour was affected by the chemical constituents, cross linker and pH[140]. The swelling content and rate and diffusion of water in acrylamide sodium acrylate hydrogel were measured by Kipcak and colleagues.[141] To ensure good swelling characteristics, the pH during gelation as well as the pH of dispersion media should be considered as they affect the swelling behaviour of hydrogels. Mesh size calculation based on the equilibrium swelling ratio of thermal protein hydrogel and time-dependent gravimetric swelling ratio indicated that the pH during gelation strongly influenced its swelling behavior.[142] The introduction of a binary solvent system (water/methanol) induces swelling behavior

of PNIPAM hydrogel and caused re-entry of liquid into the hydrogel which resulted from competitive hydrogen bonding of both solvents with polymer.[143] Thus, the swelling behaviour could be controlled with ease. Swelling characterization and equilibrium swelling kinetic studies were conducted by Ehrenhofer and colleagues.[144] Several other studies also confirmed that from synthesis to application, pH-dependent swelling played a key role in stabilizing the gel network and its overall sensing performance.[128-129]

Biomimetic activity and biocompatibility. Preserving the catalytic activity of bioreceptors is critical in biosensors to ensure rapid, accurate and highly sensitive detection of analyte. As the activity of bioreceptors depends on their native conformation, it is crucial to maintain its' innate structure and reaction favorable environment. However, maintaining the native conformation outside a living cell is challenging. At this point, the biomimicry feature of hydrogels has appeared as a great solution. The tissue resemblance and cellular environment alikeness of hydrogels provide the most favorable conditions for bioreceptors to react accurately. Outstanding performance and application in tissue engineering, regenerative bone and cartilage printing, wound dressing and healing, *in-vivo* drug delivery, microenvironment alikeness mak hydrogels' excellent biomimicry.[145–153] Another important feature is the biocompatibility of hydrogel which has improved the functionality of implantable biosensors to allow real-time monitoring of analyte concentration *in-vivo*.[154–156] These biocompatible sensors do not evoke inflammation, immune response and avoid the generation of ROS, thus causing no potential toxicity in living cells. Implanted biosensors consisting of hydrogels also degrade easily after completing their lifespan.

Rheology. Rheology is defined as the ability to flow for a liquid and the extent of deformation for a solid. Due to their inherent viscoelasticity, it is important to consider the rheological properties of hydrogels during fabrication. To explore the viscoelasticity of a hydrogel, its rheology (the flow property of materials) that measures the storage modulus G' and loss modulus G'' requires to be studied. Through rheological characterization, the flow and deformational behaviour of hydrogel have been investigated. The viscoelasticity measurement shows to what extent the viscosity dominates over elasticity. The ratio of shear strain to applied shear stress shows the degree of time-dependent

deformational change. Crosslinking density affects viscoelastic response. Low crosslinking imparts a low level of elasticity, while high crosslinking shows the opposite. In addition to the crosslinker, filler contributes to modulating the viscoelasticity of the hydrogel matrix. At low temperatures, hydrogel becomes glassy and with the increase of temperature, it becomes rubbery. Gradually decreasing elastic modulus and increasing viscous modulus. Over the course of gelation, viscoelasticity changes. The gel stiffness depends on storage modulus (G') and loss modulus (G''). When $G' > G''$, the hydrogel is predominately elastic. In contrast, when $G'' > G'$, it remains viscous. Rheological studies of various hydrogel systems reveal the feasibility of tailoring hydrogels for biosensing applications.[157–166] Various rheological tests should be considered to certify hydrogels for biosensor construction, including creep compliance, stress relaxation, strain sweep test, temperature sweep, small amplitude oscillatory shear test (SAOS) and so on. Creep compliance test reveals the tolerance of the material upon a continuous static load. In the stress relaxation test, strain is applied to measure the stress exerted by the system. The temperature sweep test is specifically important for biosensing applications since it reveals the structural deformation by measuring storage moduli and loss moduli of hydrogel through a wide range of temperatures, including the phase transition period. SAOS test is used to quantify the gel kinetics of the hydrogel revealing that during the time of gelation (Δt_{gel}), viscoelasticity properties change drastically and this needs to be considered during the construction of a biosensor.

4. Hydrogel as Bioelectrode and Biosensor's Surface Matrix

Signal transducer. The translation of non-electrical physical changes in the hydrogel system (phase transition, swelling, volume collapse) upon stimuli to detectable electrical changes is achieved by the bioelectrode/transducer. Hydrogel-based electrodes have enhanced signal transduction capacities. Conductive hydrogel facilitates electrolyte/electrode interface and favours rapid electron transfer within the hydrogel system.[167] A more precise signal generation can be achieved by entrapping redox enzymes in conductive hydrogel polymers. Moreover, carbon-based additives, such as graphene and CNTs can augment the conductivity and electrosensitivity of conventional hydrogels. Under the

domain of bioelectronics, hydrogels have been extensively studied by many researchers with the main focus on improving their conductivity. Hence, in recent years, they find increasing applications in supercapacitors, electrodes, FETs and logic circuits.[168–174] A polyacrylamide sodium casein-carboxylmethyl chitosan hydrogel transducer for motion sensing was developed by Wang and co-workers. They reported the impressive electrical conductance of this hydrogel by measuring the resistance through AC impedance method followed by conductivity calculation. The incorporation of free ion-generating compounds, such as sodium casein and carboxymethyl chitosan resulted in an efficient bio-electrode/transducer and along with mechanical stretching, the hydrogel scaffold allowed for adequate energy dissipation. Another novel bioelectrode was proposed using the combination of redox carbon nanoweb hydrogel and CP,[175] which resulted in a significantly larger current conduction than conventional electrodes. Electroactive hydrogel has also been used as a coating for bio-electrodes.[176] A hydrogel gate FET for real-time glucose monitoring was developed recently.[177] The incorporation of oxygen-absorbing metal-organic-framework zeolitic imidazolate framework-8 (ZIF-8) into conductive PAni hydrogel through nanoarchitectonics enhanced the overall electrical conductivity and allowed this composite to function as a bio-based transducer.[178]

To achieve the highest tailorability, hydrogels have been modulated and interfaced with glassy carbon electrodes, optrode and piezoelectrodes. Interfacial nanoarchitectonics increases the compatibility between hydrogel network and conventional transducer. However, studies on ion-conductive hydrogels have focused more on tailoring the hydrogel as an independent transducer, thus omitting the necessity of conjugating an external electrode as the transducer. Nanoarchitectonics enables more structural modulation which favors the production of these types of bio-based transducers. Hydrogels hold the potential to replace conventional electrodes and optrodes can be replaced by fluorescent, chemiluminescent and Raman probe-incorporated hydrogels. CP hydrogels and nanocomposite-integrated hydrogels should be investigated more rigorously to improve their conductivity. We emphasize this fact because this integration can lower manufacturing costs and overcome the drawbacks of electrochemical biosensors. In addition, photon-transferring signal

generation (chemiluminescence, fluorophores, quenching strategies) facilitates naked-eye detection and will reduce the need for additional electric potential measuring devices.

Bioreceptor immobilizer. Bioreceptors (*e.g.*, enzymes, antibodies, aptamers, DNA motifs) are the crucial components in a biosensor. The catalytic activity of these bioreceptors depends mostly on microcellular environments. Due to its high biomimetic activity and bio-affinity, hydrogels have attracted great interest as the immobilizer matrix or biosensor's surface matrix. Enzymes and other bioreceptors can be immobilized by various strategies, including physical adsorption, entrapment, covalent crosslinking, electrodeposition, and molecular printing.[179,180] The efficiency of enzyme immobilization is one of the determining factors for precise biosensing. Various novel immobilization techniques have been reported so far. Magnine and colleagues reported comparative results of three enzymes immobilized into the chitoXen matrix (combining matrix of chitosan and xanthan polymer).[181] They also performed a kinetic test to determine the stability of entrapped enzymes. Similarly, lipase was immobilized into porous ChitoXen beads and this immobilization enhanced the catalytic activity of lipase.[182] Using anionic surfactant gelation, enzyme immobilization has been achieved into chitosan capsule and the loading efficacy has been measured.[183] Kim and colleagues developed an optical biosensor by co-immobilizing conjugate enzymes and fluorophores into PEG hydrogel microparticles where 70% catalytic activity was successfully retained.[25] In another approach, where Lac enzyme was immobilized into a PEG hydrogel, successful retainment of the original catalytic activity was achieved.[184]

5. Hydrogel Nanoarchitectured Biosensor Construction

The sensing process of any biosensor is initiated by the presence of a bio-analyte or stimulus that is captured by the bioreceptor (*e.g.*, enzyme, aptamer) thus, generating a signal which is read out by the transducer. The underlying chemistry of sensing indispensably depends on the native conformation of the bioreceptor and assurance of reaction favorable conditions. The conjunction of analyte-receptor results in signal generation, in which the hydrogel collapsed and becomes assembled and swollen. These physicochemical changes are being governed by the inherent thermodynamical and rheological properties of the hydrogel. To transduce a signal that confirms the detection, either additional

transducers are interfaced with the hydrogel or a conductive hydrogel is used. One of the main shortcomings of conventional hydrogels is their impedance on interfacing electrodes, brittleness, poor conductivity and minimal interfacial environment manipulation within layers. With the emergence of bottom-up fabrication and nanoarchitectonics, these bottlenecks are being addressed.[185] Being able to control the interfacing environment would advance fabrication and this can be achieved by nanoarchitectonics-directed fabrication strategies. Self-organization, layer-by-layer assembly, and Langmuir-Blodgett (LB) strategies result in asymmetric, vectorial, and hierarchical structures. Additionally, nanoarchitectonics routinely exploits DNA assembly, peptide assembly, metal-organic framework chemistry, and coordinating polymer's modulation strategies to achieve superior functionality. Interfacial nanoarchitectonics delicately balance air-water and solid-liquid interfacial layers within a biosensor which are critical for constructing robust and ultrasensitive biosensors. The advent of CP hydrogels makes biosensors less dependent on graphene, CNT or other conductive materials. They are being used extensively in "*in-vivo* sensing" as biocompatible hydrogels do not exert cytotoxicity or immunogenicity. In the following section, the underpinning chemistry and physicochemical behavior of specific hydrogel systems will be discussed in depth.

5.1. Enzyme-based Hydrogel Biosensor

GOx-based glucose sensors often suffer from enzyme vulnerability *in vitro*. To address this, Zhai and colleagues designed PtNPs-incorporated PAni hydrogel to provide a conductive matrix for GOx immobilization and PtNPs electrochemically oxidized H_2O_2 to detect potential.[186] PAni hydrogel works as a conductive matrix that retains the efficacy of enzymes, provides large surface area and facilitates electron transfer. The assay obtained a low detection limit of 0.7 μM in the linear range between 0.01 and 8 mM. The development of low-cost, reusable and simple glucose sensor is important for managing many health conditions, including diabetes. Kim and co-workers developed a simple reusable, ratiometric glucose biosensor composed of polyacrylamide, fluorescein and rhodamine B.[187] In this assay, the conversion of glucose to glucuronolactone coupled with peroxide generated oxygen and proton, which changed the solution pH. This subsequently changed fluorescein

and rhodamine color (green to orange). The color intensity was proportional to the concentration of glucose. This hydrogel system could be regenerated and reused up to four times.

The conventional way to build a biosensor is to detect one analyte by encapsulating one receptor. However, the co-encapsulation of multiple receptors makes it possible to detect multiple analytes without affecting efficacy. In 2011, Kim *et al.* designed a photoluminescent peptide hydrogel N-fluorenylmethoxycarbonyl diphenylalanine (Fmoc-FF) to detect both glucose and hydroquinone (**Figure 5a**).[188] In this work, GOx and HRP enzymes were co-encapsulated into the hydrogel matrix which was embedded with CdTe and CdSe QDs. These QDs were used to donate an electron to the quenching agent (an electron acceptor) generated from the analyte-receptor reaction. Enzymatic catalyzation of analytes generated quenching agents that accept an electron from these QDs, leading to a reduction in photoluminescence intensity. Yuan and colleagues also reported a similar approach using a quantum dot hydrogel matrix to encapsulate tyrosinase enzyme for detecting dopamine.[189] Due to their superior biocompatibility and low toxicity, hydrogel-based biosensors have been proven to be applicable for *in-vivo* sensing. GOx-immobilized redox hydrogel for *in vivo* glucose monitoring was previously designed by Linke and colleagues.[155] They implanted glucose electrodes into the subcutaneous tissue of a dog to determine the cytotoxicity. They found the growth and development of the cell lines were not affected. Another implantable glucose sensor was designed by Quinn and co-workers that showed no immunogenicity or inflammation after implantation in rat's subcutaneous tissue for 7 days.[190] However, these *in vivo* glucose sensors are prone to degradation by ROS *in-vivo*. To overcome this limitation, Sawayama *et al.*, designed a fluorescent *in vivo* glucose biosensor entrapping two antioxidant enzymes, namely superoxide dismutase and catalase.[154] These enzymes prevented the degradation of the sensor by ROS, thereby preserving fluorescent intensities. This sensor lasted for 28 days in the rat's body with no sign of toxicity. Histopathological examination of the liver tissues supported the cytocompatibility of these three enzymes. Crumbliss and colleagues reported the detection of cholesterol by entrapping three enzymes (cholesterol esterase, cholesterol oxidase and HRP) in carrageenan hydrogel.[191][192] Enzymatic catalysis of cholesterol yielded hydrogen peroxide which was further oxidized by HRP and generated an electrical signal. Hydrogel

here played a role as an immobilization matrix for sustaining the native conformations and catalytic activities of the three enzymes. Based on the urea-urease specificity, a pH-sensitive PAA-co-dimethylaminoethyl methacrylate hydrogel was designed (**Figure 5b**).[192] Urease was entrapped into the hydrogel matrix. It catalyzed urea resulting in an alkaline environment. Consequently, the hydrogel became swollen and the increased swelling pressure was detected by the piezoresistive sensor. The detection range was reported to be 1 to 20 mmol/L.

5.2. Antibody-based Hydrogel Biosensor

Exploiting the high specificity of antigen-antibody interaction, immunosensors have been developed to detect cancer biomarkers, antibiotics, and carbohydrate antigens.[193–195] Like enzyme encapsulation, hydrogel is also an excellent immobilizing matrix for antibodies. A wide variety of tumor biomarkers, including tumor necrosis factor, prostate-specific antigen (PSA), human IgG were detected using hydrogel immunosensors. The mechanistic scheme for detecting analyte presence by immunosensor is comprising the signal (mostly second wave voltammetry, (cyclic voltammetry (CV) and differential pulse voltammetry (DPV)) before and after the addition of an antigen. Wang and colleagues designed a conductive hydrogel-based electrochemical immunosensor to detect neuron-specific enolase (NSE), a lung cancer biomarker.[196] The hydrogel film was prepared by crosslinking of 1,3,5- benzene tricarboxylate and Fe^{3+} ions and this film were further coated onto GCE and AuNPs were electrochemically deposited into the surface coupled with anti-NSE. The detection range was reported to be 1 pg mL^{-1} to 200 ng mL^{-1} and the LOD was 0.26 pg mL^{-1}. This immunosensor was also reported to resemble enzyme-linked immunosorbent assay (ELISA)-based detection. The same group also designed another NSF immunosensor using PPy-polythionine-gold CPH where GOx was used as a doping agent.[197] Zhao and co-workers proposed a sandwich-type impedimetric immunosensor made of AuNP-$CaCO_3$ triggered pH-responsive sodium alginate hydrogel to detect PSA.[198] Another PSA immunosensor was designed by Li and colleagues using a redox hydrogel consisting of aniline and vinyl ferrocene.[199] To detect ferritin in serum, an agarose hydrogel immunosensor was fabricated onto GCE by Zhang and colleagues.[200] The determination of ferritin was achieved by comparing the

DPV signal before and after the addition of ferritin solution. A colorimetric immunosensor was designed by Ma *et al.* for the detection of liver cancer marker α-fetoprotein using microcrystalline cellulose (MCC) hydrogel (**Figure 6a-e**).[201] In this report, AuNPs were loaded into the MCC hydrogel, followed by the addition of carbon nitride (g-C_3N_4) nanosheets to form porous Au@g-C_3N_4/MCC hydrogel. While the immobilization of antibody turned off the catalytic sites of AuNPs, the presence of α-fetoprotein catalytic sites generated visible color. The detection of various antigens, such as- ractopamine (by agarose gel immunosensor),[202] hepatitis B antigen (by polyacrylic hydrogel),[203] cortisol (by surface plasmon resonance (SPR)),[204] tumor necrosis factor (by ferrocene functionalized phenylalanine hydrogel have also been reported.[205]

In recent years, photonic crystals (PCs, spatially arranged periodic dielectric materials) have been integrated with hydrogels. Upon the expansion or shrinkage of hydrogel, PCs altered their photonic band gap.[206,207] Photonic crystal hydrogel (PCH) sensors are inexpensive and rapid. They allow label-free, naked-eye detection with high sensitivity. In conventional antibody-immobilized PCH biosensors, target molecules are directly bound into the hydrogel. To obtain a specific detection, this type of biosensor requires precise control and changes of hydrogel volume, charge and osmotic pressure. This sensor design is limited to the detection of larger biomolecules, and it is fabricated by immobilizing a target-binding molecule directly into the hydrogel macromolecules and cells or highly charged small ions or molecules. This strategy also depends on the enzyme's ability to undergo a substrate reversible process. It is also prone to significant interference by buffers and other species present in the sample. In many cases, naked-eye detection is not possible because of a small deformation or a color change of the PCH. Very recently, a "competition"-based PCH biosensor was design using noncovalent "crosslinked" hydrogel immobilized with both antibody and antigen (**Figure 6f**).[208] As shown in Figure 6f, in this sensor design, acrylated antibody-antigen immobilized hydrogel stayed "contracted". Upon the addition of the analyte, competitive displacement occurred, leading to the breaking of "crosslinked" hydrogel, resulting in a reversible expansion that solely depended on antibody recognition, not in size or charge of the target (antigen). Moreover, this sensor experienced large wavelength shifts upon analyte binding with minimal background noise and

excellent reversibility. This report studied the three well-known interactions [*e.g.*, IgG–Protein A (PrtA), anti-(L-glutathione reduced) antibody (Ab^{GSH})–GSH, and anti-biotin antibody (Ab^{biotin})–biotin].

5.3. Aptamer-based Hydrogel Biosensor

Owing to their selective binding, high specificity, molecular recognition and stimuli-responsive intrinsic properties, molecularly engineered aptamers are frequently used as bioreceptors to detect a wide variety of molecules. DNA aptamers are used in hydrogels as crosslinkers to recognize the target as well as to generate signals. For instance, aptamers act as conventional DNA crosslinkers in the absence of a target, whereas in the presence of the target, they preferentially form a complex with the target to induce a structural change in the hydrogel.[122,209] Such hydrogel utilizes programmable features of both DNA components and short aptamer sequences to produce signals. Aptamersin hydrogels also act as highly specific bioactive groups or tags to bind target molecules, resulting in the release of preloaded molecules to generate signals.[210] Based on these intrinsic features, aptamer-based hydrogels can be easily integrated with several signalling mechanisms, such as colorimetry, fluorescence and SPR to create rapid and sensitive biosensors for the detection of disease biomarkers. Zhu and colleagues proposed a colorimetric protocol of aptamer-based detection.[211] In this design, two DNA polymer strands (PS-A and PS-B) that were complementary to an adjacent area of a DNA aptamer sequence were mixed to form a transparent liquid (**Figure 7a**). Upon the addition of an aptamer "linker-apt", both strands A and B hybridized with the aptamer to initiate the crosslinking of linear polyacrylamide polymers, thus increasing the viscosity of polymers to form a gel and trapped the previously added enzyme. With the addition of the target, the aptamer binds with the target through a competitive target–aptamer binding, thereby reducing the crosslinking density. In turn, this released the trapped enzyme for subsequent catalytic signal amplifications to generate a change in the substrate color, thus enabling visual detection. Jung and colleagues proposed a colorimetric detection of Ochratoxin A by AuNPs-associated aptamer.[212] Polyacrylamide strands, AuNPs and aptamer formed hydrogel which collapsed with the introduction of Ochratoxin A to produce a red-colored

solution. Following a similar approach, visual detection of mercury and adenosine was achieved by using an aptamer-functionalized hydrogel.[213] A virus responsive aptamer hydrogel was designed to enable naked-eye detection of apple stem pitting virus.[214] Avian influenza virus has been successfully detected using a quartz crystal microbalance aptasensor. Specific aptamer for AIV H5N5 strain was obtained by SELEX, where 200 μL of the target AIV was detected and analyzed by dot blot assay.[215]

Aptamers also undergo conformational switches upon binding with the target, making them ideal recognition element to design nanoscale biosensors with a wide range of signal readout techniques.[216] The conformational change of immobilized aptamers alters the distance between the signal molecules and the transduction surfaces, which has a significant impact on the generated ON-OFF signals.[217] DNA-based hydrogel utilized this intrinsic property to detect RNA based-disease biomarkers. He and colleagues reported a Raman probe-incorporated 3D DNA hydrogel for ultrasensitive detection of miRNA.[218] The prepared SERS probe employed ficus viren leaves, Nafion and silver nitrate (leaf@Nafion@$AgNO_3$). For preparing the DNA hydrogel, they used two strands of acrydite-modified DNA and DNA linker strand for crosslinking. The assembled DNA hydrogel on the leaf remained on signal "OFF" state and upon the presence of miRNA, the hydrogel disassembled and switched to "ON" state. Hydrogel-based qPCR (quantitative polymerase chain reaction) for Alzheimer disease detectionhas been developed.[219] Chapin and colleagues have achieved sub-femtomolar sensitivity for miRNA detection where they quantified multiplex miRNA and encoded them into the hydrogel matrix.[220]

When the target molecules are recognized, the crosslinking density of the aptamer hydrogels is significantly altered, leading to dramatic changes in volume and water content. This excellent property can solve the issues encountered in Terahertz (THz)-metamaterial-based biosensing. In THz-sensing, the target molecules should be dried on in a low-adsorption medium or dried.[221] An aqueous environment is not favorable for this sensing process as it generates strong THz absorption (~240 cm–1 at 1 THz) and severely obscures the response of solute molecules.[222] On the other hand, due to the mismatch between the wavelengths of the THz waves and the size of the molecules, THz

spectroscopy could only generate a limited absorption signal from a dried surface. THz metamaterials functionalized with aptamer hydrogels may be able to detect tiny target-induced changes in the hydration state of hydrogels, which is promising for constructing a molecule-specific THz biosensor that can be used in an aqueous setting. Recently, a molecule-specific THz biosensor was fabricated from an aptamer hydrogel-functionalized THz metamaterial for the sensitive detection of thrombin.[223] In this sensor, the aptamer and its complementary sequence were grafted onto the MBAA cross-linked linear polyacrylamide polymer to prepare an aptamer hydrogel containing a hydrophilic and insoluble porous network structure (**Figure 7b-e**). Then, the aptamer hydrogel was tightly immobilized on the salinized THz metamaterial with a homogeneous structure to fabricate the proposed THz biosensor (**Figure 1c**). The self-referenced reflection measurement model was exploited to read out the signal of the THz biosensor. This THz biosensor could detect thrombin with a concentration as low as 0.40 pM in human serum.

6. Hydrogel Biosensing for Disease-Specific Biomarkers

Disease-specific biomarkers are biomolecules that can be used to diagnose and prognostically assess a disease's pathophysiological state based on their presence, absence, or fluctuation in concentration across time.[204] Because of their high specificity to disease and responsiveness only at a diseased state, they offer a precise diagnosis of diseases with a low likelihood of false positives. Moreover, diagnosis of diseases based on biomarker detection has become advantageous as it is non-invasive, can detect minimal residual disease, and shows a lower limit of detection (LOD) than conventional diagnosis methods, such as ELISA, PCR, high-pressure liquid chromatography (HPLC), imaging method, solid biopsy, *etc*. A broad spectrum of disease-specific biomarkers is well characterized, including biochemicals, metabolites, nucleic acids, proteins, antibodies, bacterial enzymes, disease-specific genes, extracellular vesicles, exosomes, circulating tumor cells and so on (**Table 1**)[264-274]. Since the creation of the receptors of these biomarkers has effectively retained in the hydrogel network compared to other polymers, hydrogel-based biosensors for detecting disease-specific biomarkers have become increasingly popular.[212] Considering the significance of disease-specific

biomarkers and the emergence of hydrogel in fabricating biosensors, the upcoming section elaborates on the recent advancements of nanostructure-integrated hydrogel-based biosensors for detecting disease-specific biomarkers, such as DNA, RNA, protein, cells, and extracellular vesicles.

6.1 DNA Biomarker Sensing

DNA biomarker-based detection has become crucial in cancer diagnosis and prognosis as it offers a significant amount of variety in genetic makeup that could lead to the development of personalized diagnosis and prognosis. Cancer has been characterized by two types of DNA biomarkers so far, namely circulating tumor DNA (ctDNAs) and methylated tumor-specific DNA. Since various types of cancer have been reported to circulate distinct DNA biomarkers, DNA-based detection method has surpassed conventional imaging-based methods, such as MRI, CT-Scan, and solid biopsy for cancer diagnosis.[224 - 226] Given the importance of early-stage detection in eradicating cancer, DNA biomarker-based diagnosis becomes increasingly crucial as it offers a non-invasive way of detection, low detection limit, and rapid analysis. DNA biomarker-based detection employs the specificity of Watson crick base pairing. Therefore, aptamers, molecular beacons, and synthetic DNAzymes have been used as receptors for DNA biomarkers, collectively known as DNA nanomachines, *i.e.*, nanoscale oligonucleotide complex. DNA nanomachines have been synthetically built to be sensitive towards DNA biomarkers.[227] Similar to other biosensors, retaining the native conformation of DNA nanomachine receptors for optimizing the catalytic activity is crucial for achieving ultrasensitive detection and this can be achieved by utilizing hydrogels. Besides this scaffolding purpose, hydrogels are also utilized for qualitative analysis and leveraging electrochemical signal transduction where DNA itself is assembled to form a macroscopic hydrogel network.

Nanostructures-integrated hydrogels have gained significant attention for DNA biosensing. For instance, Baeissa *et al.* integrated AuNPs with a DNA-functionalized monolithic hydrogel to obtain the colorimetric detection of a DNA sequence.[129] In this strategy, two kinds of probe DNA molecules were utilized; where one is modified with an acrydite to attach to the polyacrylamide hydrogel matrix and the other is modified with 3′-thiol for attachment to AuNPs (**Figure 8**). When the

target DNA was added, the AuNPs were linked to the hydrogel surface to produce a red-colored hydrogel. The sensitivity was further increased by using the AuNPs as a catalyst for the reduction of silver ions to metallic silver to give a black color. This approach could detect 1 pM of DNA by integrating both transparent hydrogel (which generated a very low background signal) and AuNPs with a high extinction coefficient as a catalyst. A similar strategy was also reported where photonic QDs were tagged to prepare DNA responsive hydrogel beads.[228] Upon the hybridization of the target DNA with the crosslinked single-stranded DNA in the hydrogel grid, the hydrogel shrank and this led to a blue shift in the Bragg diffraction peak position of the beads, thus facilitating the quantitative estimation of DNA.

In addition to detecting cancer biomarkers, the detection of Alzheimer disease has been achieved utilizing DNA hydrogel as a scaffold for retaining alkaline phosphatase activity that leads to the disassembly of DNA, Alzheimer disease-specific biomarker.[229] DNA hydrogel has been used for developing point-of-care devices, such as the personal glucose meter proposed by Gao *et al.*[230] Stating the drawbacks of conventional paper-based colorimetric assay of a glucose meter, they have drawn the significance of DNA hydrogel in interlocking enzymes as conventional assay suffers from lower sensitivity due to the adsorption of enzymes on a solid surface which did not occur when using DNA hydrogel. Besides detecting biomarkers on blood, the interstitial fluid serves as a rich source of biomarkers that can be used for detecting cell-free DNA. This has enabled the fabrication of microneedle coated with alginate peptide.[231]

6.2 RNA Biomarker Sensing

RNA biomarkers have been intricately linked to cancer pathogenesis, and they can be identified in a low quantity that significantly reduces the risk of false negatives. Well-known disease-specific RNA biomarkers have been identified, such as microRNA (miRNA) PAM50 for breast cancer,[232] miRNA-21 for pancreatic cancer,[233] PiwiRNA-651 for Hodgkin lymphoma,[234] snoRNA for lung cancer[235] and so on. Because of their higher specificity than DNA biomarkers, RNA biomarker detection can provide a more precise and accurate cancer diagnosis and prognosis. Conventional RNA biomarker

detection has been performed by high throughput RNA-seq and qRT-PCR technologies. Owing to cost inefficiency and significant time consumption, RNA biomarker detection by RNA-seq or qRT-PCR might not be available for rapid detection. That being the case, an RNA biosensor for detecting disease-specific RNA biomarkers may be efficient, though it is still under investigation.

The principle of RNA sensing exploits the same nucleotides as DNA sense does. Typically, self-assembled DNAzyme hydrogel acts as an identifier in sensing RNA biomarkers. Micro-RNA responsive DNA hydrogel was developed by utilizing AuAg NPs as SERS tags, making detection of multiple miRNAs possible (**Figure 9**).[236] Responsive DNA hydrogel was assembled where multiple nucleic acid components (MNAzyme) act as an identifier. MNAzymes formed an inactive DNAzyme motif and a target miRNA-responsive DNA hydrogel with an "OFF" status. Hence, the AuAgNPs SERS tags could not pass through the hydrogel to be captured by the streptavidin-modified detection area, resulting in weak or no Raman signal. Upon the presence of target miRNA, the conformation and activity of the relative MNAzyme were restored and thus, MNAzyme showed specificity toward the target miRNA. The DNA hydrogel network became disintegrated, enabling AuAgNPs SERS tags to be captured by streptavidin detection for target-specific Raman signal.

In-situ DNA hydrogelation for miRNA detection has also been developed utilizing AuNPs and isothermal catalyst terminal deoxynucleotidyl transferase (TdT) that catalyzed the coupling of deoxynucleotide triphosphates (dNTPs) for the formation of DNA hydrogel. This hydrogel network could detect miRNA as a cancer biomarker (hsa-let-7d-5p).[237] Hydrogel sensing motif has been patterned on a fibrous substrate for miRNA detection.[238] Similarly, a 3D hydrogel-based on chitosan and carbon dots (CDs) has been developed for breast cancer detection using a miRNA-21 biomarker.[239] In their work, the carbon dot-chitosan nanocomposite hydrogel was prepared as a biosensor scaffold. The interaction between DNA probe and target microRNA resulted in network disintegration and the signal was detected by utilizing a fluorophore. Very recently, we have reported hydrogel-functionalized surface-based transducers that integrated 3D micro- or macrostructure of κ-carrageenan hydrogels into a mesoporous Au platform to obtain a favorable moiety for promoting higher miRNA adsorption.[240] The κ-carrageenan gel provided a 3D porous network on Au electrode

surface to enable higher adsorption of target miRNA for CC interrogation of miRNA in presence of a redox molecule-ruthenium hexaammine (III) chloride. The enhanced miRNA adsorption and electrocatalytic activity of mesoporous gold electrode (MPGE)/gel led to attomolar (50 aM) level of detection of miRNA with a dynamic range from 100 pM to 10 aM. This type of biosensor has a promising potential for translation into precision-controlled sensing devices for contemporary clinical demands.

6.3 Protein Sensing

Protein biomarkers, as a distinguishing signature of pathology, serve not only as diagnostic and prognostic indicators but also as pharmacological targets as part of the personalized medicine research, because proteome profiles differ among individuals. Protein biomarkers depict the pathophysiological picture relatively better than genetic biomarker profiling. Protein biomarker detection has generally been conducted by expensive instrumentations, such as MALDI/MS, ELISA, HPLC, SPR , PET (positron emission tomography), *etc*. These expensive diagnostics have been replaced by quick, low-cost microfluidic sensor chips. Furthermore, the utilization of HRP mimicking nanozyme in an immunosensor reduces costs significantly, while the use of a hydrogel for maintaining the original structure of antibody can provide high specificity and sensitivity.[241–243] Protein biosensors rely on the immune interaction of antibody and antigen where the protein of interest acts as an antigen and captures antibodies serving as an identifier. In developing immunosensors, hydrogel plays a crucial role in preserving antibody's conformation intact as well as providing large surface area, high porosity and biocompatibility.[244] An aptasensor has also been fabricated using AuNPs embedded inside hydrogel for thrombin detection.[245] PVA-borax hydrogel with embedded AuNPs was previously synthesized on which thiolated thrombin binding aptamer with high sensitivity to thrombin was attached. Signal readout has been achieved by Resonance Rayleigh Scattering (RRS). There is an interesting report where tunable plasmonic nanostructures of AuNPs were self-assembled onto a solid SERS substrate and subsequently transferred onto a PAA gel for the detection of hemoproteins (**Figure 10**).[246] This substrate possesses reversible plasmonic spectral

shifts which are dependent on the salt concentration due to relative changes in the gap distances between AuNPs. Upon the addition of the target protein, the substrate transfer from open to closed form and enhanced SERS signal was generated. This active gap control *via* volume change in the hydrogel could improve SERS signals by improving insertion efficiency with wider gaps and decreasing the gap distance for developing hot spots at the time of detection.

The 3D network of nanostructured conducting hydrogel also facilitated the ions and electron transport to enhance conductivity and greater effective surface area for increasing the number of immobilized biomolecules. For instance, a hydrogel comprising AuNPs on PPy hydrogel was reported for the electrochemical detection of Carcinoembryonic antigen (CEA).[105] The 3D nanostructured PPy hydrogel performed crucial roles in the dispersion of AuNPs, which worked as the biomolecule immobilization matrix and provided an electrically continuous 3D route for efficient charge collection. This immunosensor was able to detect a wide linear range of protein from 1 fg mL^{-1} to 200 ng mL^{-1}] with an ultralow LOD of 0.16 fg mL^{-1}. In another report, a nanostructured conductive hydrogel prepared by the crosslinking coordination method using benzene tricarboxylic acid as the ligand and Fe^{3+} as the metal ions was reported for neuron-specific enolase (NSE) marker.[196] In this report, GCE was modified with the hydrogel film followed by electrodeposition of AuNPs for anchoring anti-NSE antibody for target NSE binding.

6.4 Cytosensing

Circulating tumor and cancer cells can also serve as biomarkers owing to the overexpression of epithelial cell adhesion molecules (EpCAM) on the cell surface, differentiating them from healthy normal cells. Moreover, as various cancer types have been distinguished with various cancer cells, whole cancer cell sensing has provided precise cancer diagnosis, prognosis, and theranostics. In clinical practice, cancer cytosensing has been established with the development of cancer cytosensors for prostate tumor cell (Du-145),[247] ovarian cancer cell (HeLa cell),[248] breast cancer cell (MCF-7),[249] and non-small lung cancer carcinoma (A549) detection.[250] Cytosensing utilized antibody-antigen interaction and aptamer-based detection where overly expressed cell surface proteins act as an

antigen, and an antibody or aptamer labelled them for readout. Many cytosensors have been designed and fabricated in microfluidic chips or other scaffolding platforms attached to some signalling techniques. Despite the wider applicability of these cytosensors, they struggle to retain cellular stability. This can be resolved by introducing a 3D hydrogel to minimize cell damage.[251] This is because DNA hydrogel mimics extracellular matrix, thus the cell viability and molecular integrity can be preserved. The NPs can be coated onto the gel to provide or further strengthen the conductivity of the hydrogel and increase the specific surface area of the cytosensor. For example, chitosan hydrogel coupled with carbon nanofiber (CNF) was electrodeposited to achieve a conductive architecture for K562 cell attachment.[252] Chitosan hydrogel provided biocompatibility and adhesion, whereas CNF served as an electron conductor, promoting electrochemical (impedimetric) cytosensing.

The electrodeposited conductive architecture demonstrated high compatibility for cell adhesion by combining the biocompatibility and good adhesion of chitosan with the unique features of nanoscale carbonaceous materials.[253] Hao *et al.* constructed a cytosensor by electrodepositing chitosan and carbon nanofiber (CNF), where chitosan provided the biological moiety for cell adhesion (K562 cells as a model) and CNF provided enhanced conductivity and catalytic activity.[252] This design increased the electron transfer impedance of the transduction surface, leading to the formation of an impedance cell sensor. The electrodeposited CNFhydrogel was able to adhere closely to the electrode, while retaining its inherent characteristics. This impedance sensor was able to detect K562 cells ranging from 5×10^3 to 5.0×10^7 cells mL^{-1} with a LOD of 1×10^3 cells mL^{-1}. Electrochemiluminescence (ECL) is a powerful analytical method in bioanalysis that combines electrochemistry and chemiluminescence and has a high potential for cell surface analysis. However, the cell causes steric hindrance on the electrode surface, resulting in a non-specific response[254]. This negative effect for ECL can be mitigated by using a permeable substrate that can minimize steric hindrance and give conductivity to activate the ECL probes tagged on cells. In this context, graphene-containing hydrogels are extremely promising since hydrogels provide permeability for cells, while graphene gives high conductivity on the electrode surface. For instance, a graphene hydrogel (GH)-based ECL cytosensor was reported for the quantitative detection of glucose transporter 4 (GLUT4) on the

surface of human skeletal muscle cells HSMC cells.[255] The GH was used to construct a permeable membrane on the electrode surface, and CDs labelled with GLUT4 were used to generate ECL signals (**Figure 11**). When GH interacted with cells in a sandwich arrangement, ECL emission occured due to the diffusion of the co-reactant $K_2S_2O_8$. The GH-based electrode improved accuracy and proved to be a useful tool for investigating GLUT4 expression. The prepared cytosensor performed well analytically for HSMC cells, with a LOD of 200 cells mL^{-1}. The average GLUT4 concentration per HSMC cell was calculated to be 1.88×10^5.

ECL is also present as a potential-resolved ratiometric form, where the quantification depends on the ratio of two signals. This strategy fulfils the requirement for multi-target analysis, and thus, it is an ideal approach to eliminate the interference factors and make the detection more convincing. Based on conductive hydrogels, ratiometric ECL was also reported for the quantification of cancer cells.[256,257] For instance, a three-channel ratiometric ECL method was proposed for MCF-7 cell analysis by combining PAni hydrogel and three potential-resolved nanostructured ECL probes, *e.g.*, g-C_3N_4, luminol-functioned AuNPs (Lu–Au NPs), and $Ru(bpy)_3^{2+}$-doped silica NPs ($RuSiO_2$ NPs)[257]. The MCF-7 cells were labelled with HA-$RuSiO_2$ NPs and the epidermal growth factor was functionalized with g-C_3N_4 (EGF-g-C_3N_4). These two electrodes provided signals in presence of co-reactants $K_2S_2O_8$ and TPA. A cytosensor of this type provides a multichannel ECL approach to boost throughput, allowing ECL to be used for cellular immunoanalysis.

6.5 Extracellular Vesicle Sensing

Extracellular vesicles (EVs) come in a variety of exosomes, ectosomes, microvesicles which act as shuttles for cargo molecules, supporting crosstalk between cells which has increased in the cancerous state.[258] The cargo molecules inside these vesicles reflect the real cellular microenvironment in a diseased state as a significant difference has been observed between EV secreted by cancer cell and healthy cell. Moreover, the quantitative difference of EVs between diseased and healthy cells substantiates the significance of EV sensing in cancer detection and prognosis.[259,260] Like other biomarker detection, EVs (*e.g.*, exosomes) are also being sensed by exploiting the specificity of

antibody and aptamer, where antigens on the vesicle surface are detected by these receptors. Due to the cellular resemblance, hydrogel microchips for immobilizing bio recognizers have been developed. Hydrogel microchip embedded with antibodies for detecting tetraspanins and prognostic markers of colorectal cancers has been proposed.[261] Methylacrylamide monomer and antibody were copolymerized by the UV initiator and the antibody-tethered hydrogel biochip could detect disease-specific exosomes. Signal readout has previously been achieved by an immunofluorescent assay. Chen *et al.* proposed hydrogel-AuNP supramolecular sphere (H-Au) for detecting exosomes obtained from prostate cancer cells using surface plasmon resonance imaging and magnetic bead-based detection.[262] In this strategy, hydrogel acted as a scaffold for retaining exosome viability, and the embedded AuNPs helped to attract DNA linkers, aptamers, and other DNA probes. With the integration of both the signal amplification effect of hydrogel and the LSPR effect of AuNPs, this SPR imaging (SPRi) biosensor exhibited a wide linear range of exosome detection with a LOD of 1.00×10^5 particles mL^{-1}. The surface plasmon resonance imaging offered distinguishable changes in the resulting refractive index, thus favoring a straightforward detection. The number of disease-related EVs or exosomes is relatively low compared to non-diseased EVs or exosomes. Furthermore, they are small and exist in body fluids with competing matrix components, necessitating EV enrichment and isolation before detection. To circumvent this, hydrogel microparticles (MGs) were created by encapsulating CuS NPs in a hydrogel created by copolymerizing acrylic acid, allylamine, and N-isopropyl acrylamide (**Figure 12**).[263] The microgels allowed for in-situ EV extraction *via* membrane filtering and EV detection because they contain a high concentration of Cu^{2+} ions per particle, resulting in a strong ECL signal.

7. Conclusion and Future Perspective

The utilization of hydrogels for fabricating biosensors transduction is highly promising because of their inherent cellular resemblance which is indispensable for in-vivo sensing. The rapid signalling capacity (due to fast phase transition) and reusability (because of its reversible nature) of hydrogels can lead to high sensitivity and low fabrication cost in biosensor construction. Nonetheless, The limitations of hydrogels in reaching advanced materials functionality can be addressed with the introduction of nanoarchitectonics since it enables the properties regulation of materials by atomic/molecular level manipulation, morphological control, and cutting-edge interfacial fabrication.

This review describes the state-of-the-art fabrication of nanostructured hydrogel biosensors. The multifaceted synthesis, fabrication, mechanism of detection along with the inherent characteristics of hydrogels were discussed. Meticulous research and endeavor toward evolving robust hydrogel biosensors were epitomized. It is apparent now that the integration of hydrogels with other nanostructures (*e.g.*, carbon) and composites can enhance their biosensing performance. Carbon nanostructures, such as graphene, CNTs and other carbon materials perform meticulously in the chemical/electrochemical field but in biosensing, hydrogels surpass them because of their biomimetic and biocompatible nature. With the advent of cutting-edge engineering techniques, the applications of hydrogels become increasingly diverse. However, its end-usage is still often overlooked. While graphene and CNT hydrogels have shown promise in the biosensing field, their clinical applications are still rather limited. Other applications of hydrogels, such as wound healing, tissue engineering, organ printing, and drug delivery have benefitted at the end-user level, there is still a lack of practical point-of-care devices based on hydrogels.

This comprehensive review will provoke a second thought to biosensor researchers and industrial expertise to overcome bottom line shortcomings. It is anticipated that conductive hydrogels may potentially eliminate the need for additional electrodes thus, lowering the manufacturing cost of biosensors. We envision that the utilization of leading-edge fabrication and interfacing techniques, as well as real-time screening strategies, will overcome the challenges toward developing sophisticated, amenable, user-friendly POC biosensors. One key demand that hydrogel nanoarchitectonics can address is the stringent analytical requirements of *in-vivo* sensing. Despite showing great promise, no

single approach has been able to meet all the analytical requirements for *in-vivo* sensing. An *in-vivo* sensor with full clinical functionality should have excellent analytical attributes, such as good dynamic range, ultrasensitivity, high specificity, reversibility, fast response time, and good biocompatibility. Biocompatibility is particularly important to achieve long-term continuous and accurate monitoring of chemical dynamics of physiological analytes *in-vivo*. Hydrogel nanoarchitectonics will not only be critical for obtaining clinically relevant sensitivity, but it is also important for enhancing the specificity by providing biomimetic structure, biocompatibility, long term usability and easy readout.

There have also been substantial efforts on the development of high-throughput biosensing platforms where hydrogel nanoarchitectonics can play key roles. Although several existing high-throughput screening platforms, such as microarray has nearly met the clinical reality, portable biosensor-based high-throughput sensing still seems to be a far off task, primarily due to biofouling and absence of robust sensor surface. Commercially available materials in high-throughput sensor surfaces have disadvantages associated with improper packing leading to leakage and cross-contamination, blockage due to small pores, *etc*. The incorporation of hydrogel nanoarchitectonics in high-throughput screening can enhance the sensing performance. Whilst we now have a better understanding of existing issues in high throughput *in-vivo* biosensing platforms, there are no magic bullets. Hydrogel nanoarchitectonics-integrated sensing platforms may still require new ways of thinking about the other key components, such as device automation and better system integration through power management, wireless data transmission and obtaining clinically meaningful data.

Overall, we envision that the utilization of leading-edge fabrication, interfacing techniques, and real times screening strategies will overcome impedance towards developing sophisticated, amenable, user-friendly POC biosensors. To fully exploit the advantages of hydrogels, we need to customize starting from monomer selection to bottom-up engineering thus hydrogel undergoes subtle specialization to become a meticulous one. To tailor hydrogels for sensing purposes, emphasis should be given to various characteristics, such as encapsulating suitable receptors, perpetuating native

conformation, enhancing conductivity and mechanical strength, and promoting favorable interfacial interactions which are crucial for biosensing.

Acknowledgements

This study is supported by the JSPS fellowship to M.K.M. Y. V. K. acknowledges the financial support from Advance Queensland (AQIRF043-2020RD3). Y. Y. thanks the financial support from ARC Discovery Project (ARC DP190102944) and JST-ERATO Yamauchi Materials Space-Tectonics Project (JPMJER2003). The authors are also grateful to the Queensland node of the Australian National Fabrication Facility, a company established under the National Collaborative Research Infrastructure Strategy to provide nano- and micro-fabrication facilities for Australian researchers.

Received: ((will be filled in by the editorial staff))

Revised: ((will be filled in by the editorial staff))

Published online: ((will be filled in by the editorial staff))

References

[1] D. W. Kimmel, G. LeBlanc, M. E. Meschievitz, D. E. Cliffel, *Anal. Chem.* **2012**, *84*, 685.

[2] M. Malmqvist, *Nature* **1993**, *361*, 186.

[3] J. Kirsch, C. Siltanen, Q. Zhou, A. Revzin, A. Simonian, *Chem. Soc. Rev.* **2013**, *42*, 8733.

[4] M. K. Masud, M. Umer, Md. S. A. Hossain, Y. Yamauchi, N.-T. Nguyen, M. J. A. Shiddiky, *Trends Biochem. Sci.* **2019**, *44*, 433.

[5] K. Saha, S. S. Agasti, C. Kim, X. Li, V. M. Rotello, *Chem. Rev.* **2012**, *112*, 2739.

[6] C.-M. Tîlmaciu, M. C. Morris, *Front. Chem.* **2015**, *3*, 59.

[7] X. Zhang, Q. Guo, D. Cui, *Sensors* **2009**, *9*.

[8] M. Pumera, *Mater. Today* **2011**, *14*, 308.

[9] M. K. Masud, J. Na, M. Younus, Md. S. A. Hossain, Y. Bando, M. J. A. Shiddiky, Y. Yamauchi, *Chem. Soc. Rev.* **2019**, *48*, 5717.

[10] Y. Wang, J. Dostalek, W. Knoll, *Anal. Chem.* **2011**, *83*, 6202.

[11] Y. Wang, R. Hu, G. Lin, I. Roy, K.-T. Yong, *ACS Appl. Mater. Interfaces* **2013**, *5*, 2786.

[12] C. Jianrong, M. Yuqing, H. Nongyue, W. Xiaohua, L. Sijiao, *Biotechnol. Adv.* **2004**, *22*, 505.

[13] K. Ariga, D. T. Leong, T. Mori, *Adv. Funct. Mater.* **2018**, *28*, 1702905.

[14] T.-A. Pham, A. Qamar, T. Dinh, M. K. Masud, M. Rais-Zadeh, D. G. Senesky, Y. Yamauchi, N.-T. Nguyen, H.-P. Phan, *Adv. Sci.* **2020**, *7*, 2001294.

[15] M. Liu, Y. Ishida, Y. Ebina, T. Sasaki, T. Hikima, M. Takata, T. Aida, *Nature* **2015**, *517*, 68.

[16] J. Lee, P. W. Bisso, R. L. Srinivas, J. J. Kim, A. J. Swiston, P. S. Doyle, *Nat. Mater.* **2014**, *13*, 524.

[17] Y. S. Kim, M. Liu, Y. Ishida, Y. Ebina, M. Osada, T. Sasaki, T. Hikima, M. Takata, T. Aida, *Nat. Mater.* **2015**, *14*, 1002.

[18] L. Brannon-Peppas, N. A. Peppas, *Int. J. Pharm.* **1991**, *70*, 53.

[19] L. Brannon-Peppas, N. A. Peppas, *Chem. Eng. Sci.* **1991**, *46*, 715.

[20] N. A. Peppas, L. Brannon-Peppas, *J. Membr. Sci.* **1990**, *48*, 281.

[21] R. A. Siegel, B. A. Firestone, *Macromolecules* **1988**, *21*, 3254.

[22] I. S. Han, J. Magda, S. L. Lew, Y. S. Jean, 35.

[23] S. D. Carrigan, G. Scott, M. Tabrizian, *Langmuir* **2005**, *21*, 5966.

[24] P. T. Charles, E. R. Goldman, J. G. Rangasammy, C. L. Schauer, M.-S. Chen, C. R. Taitt, *Microarrays Biodefense Environ. Appl.* **2004**, *20*, 753.

[25] B. Kim, Y. Lee, K. Lee, W.-G. Koh, *NanoBio-Seoul 2008* **2009**, *9*, e225.

[26] H. R. Culver, J. R. Clegg, N. A. Peppas, *Acc. Chem. Res.* **2017**, *50*, 170.

[27] A. N. Dalrymple, U. A. Robles, M. Huynh, B. A. Nayagam, R. A. Green, L. A. Poole-Warren, J. B. Fallon, R. K. Shepherd, *J. Neural Eng.* **2020**, *17*, 026018.

[28] L. Li, L. Pan, Z. Ma, K. Yan, W. Cheng, Y. Shi, G. Yu, *Nano Lett.* **2018**, *18*, 3322.

[29] Q. Peng, J. Chen, T. Wang, X. Peng, J. Liu, X. Wang, J. Wang, H. Zeng, *Recent advances in designing conductive hydrogels for flexible electronics*, Vol. 2, John Wiley & Sons, Ltd, **2020**, pp. 843–865.

[30] E. M. Ahmed, *J. Adv. Res.* **2015**, *6*, 105.

[31] E. Caló, V. V. Khutoryanskiy, *50 Years Eur. Polym. J.* **2015**, *65*, 252.

[32] A. C. Daly, L. Riley, T. Segura, J. A. Burdick, *Nat. Rev. Mater.* **2020**, *5*, 20.

[33] M. Mahinroosta, Z. Jomeh Farsangi, A. Allahverdi, Z. Shakoori, *Mater. Today Chem.* **2018**, *8*, 42.

[34] D. Buenger, F. Topuz, J. Groll, *Prog. Polym. Sci.* **2012**, *37*, 1678.

[35] G. C. Le Goff, R. L. Srinivas, W. A. Hill, P. S. Doyle, *Eur. Polym. J.* **2015**, *72*, 386.

[36] F. Li, D. Lyu, S. Liu, W. Guo, *DNA Hydrogels and Microgels for Biosensing and Biomedical Applications*, Vol. 32, John Wiley & Sons, Ltd, **2020**.

[37] A. Richter, G. Paschew, S. Klatt, J. Lienig, K.-F. Arndt, H.-J. P. Adler, *Sensors* **2008**, *8*, 561.

[38] M. F. Akhtar, M. Hanif, N. M. Ranjha, *Saudi Pharm. J.* **2016**, *24*, 554.

[39] A. M. Mathur, S. K. Moorjani, A. B. Scranton, *J. Macromol. Sci. Part C* **1996**, *36*, 405.

[40] X. Li, W. Wu, W. Liu, *Carbohydr. Polym.* **2008**, *71*, 394.

[41] N. Ranganathan, R. Joseph Bensingh, M. Abdul Kader, S. K. Nayak, In *Cellulose-Based Superabsorbent Hydrogels* (Ed.: Mondal, Md. I. H.), Springer International Publishing, Cham, **2018**, pp. 1–25.

[42] S. K. H. Gulrez, S. Al-Assaf, G. O. Phillips, *Prog. Mol. Environ. Bioeng. - Anal. Model. Technol. Appl.* **2011**.

[43] W. E. Hennink, C. F. van Nostrum, *MOST CITED Pap. Hist. Adv. DRUG Deliv. Rev. TRIBUTE 25TH Anniv. J.* **2012**, *64*, 223.

[44] J. M. Yang, O. S. Olanrele, X. Zhang, C. C. Hsu, In *Novel Biomaterials for Regenerative Medicine* (Eds.: Chun, H. J.; Park, K.; Kim, C.-H.; Khang, G.), Springer, Singapore, **2018**, pp. 197–224.

[45] G. Acharya, C. S. Shin, M. McDermott, H. Mishra, H. Park, I. C. Kwon, K. Park, *Pharm. Nanotechnol. Unmet Needs Drug Deliv.* **2010**, *141*, 314.

[46] H. Fan, J. P. Gong, *Macromolecules* **2020**, *53*, 2769.

[47] J. M. Unagolla, A. C. Jayasuriya, *Appl. Mater. Today* **2020**, *18*, 100479.

[48] J. Yan, V. A. Pedrosa, A. L. Simonian, A. Revzin, *ACS Appl. Mater. Interfaces* **2010**, *2*, 748.

[49] Y. Jiang, N. Krishnan, J. Heo, R. H. Fang, L. Zhang, *J. Controlled Release* **2020**, *324*, 505.

[50] I. M. El-Sherbiny, H. D. C. Smyth, *J. Nanomater.* **2011**, *2011*, 910539.

[51] S. R. Shin, S. M. Jung, M. Zalabany, K. Kim, P. Zorlutuna, S. B. Kim, M. Nikkhah, M. Khabiry, M. Azize, J. Kong, K.-T. Wan, T. Palacios, M. R. Dokmeci, H. Bae, X. S. Tang, A. Khademhosseini, *ACS Nano* **2013**, *7*, 2369.

[52] O. C. Compton, S. T. Nguyen, *Small Weinh. Bergstr. Ger.* **2010**, *6*, 711.

[53] M. Pumera, *Electrochem. Commun.* **2013**, *36*, 14.

[54] M. J. Allen, V. C. Tung, R. B. Kaner, *Chem. Rev.* **2010**, *110*, 132.

[55] D. R. Cooper, B. D'Anjou, N. Ghattamaneni, B. Harack, M. Hilke, A. Horth, N. Majlis, M. Massicotte, L. Vandsburger, E. Whiteway, V. Yu, *ISRN Condens. Matter Phys.* **2012**, *2012*, 501686.

[56] Z. Zhao, X. Wang, J. Qiu, J. Lin, D. Xu, C. Zhang, M. Lv, X. Yang, *Rev. Adv. Mater. Sci.* **2014**, *36*, 137.

[57] H.-P. Cong, X.-C. Ren, P. Wang, S.-H. Yu, *ACS Nano* **2012**, *6*, 2693.

[58] M. Cao, J. Su, S. Fan, H. Qiu, D. Su, L. Li, *Chem. Eng. J.* **2021**, *406*, 126777.

[59] Y. Xu, K. Sheng, C. Li, G. Shi, *ACS Nano* **2010**, *4*, 4324.

[60] H. Bai, C. Li, X. Wang, G. Shi, *J. Phys. Chem. C* **2011**, *115*, 5545.

[61] Y. Xu, G. Shi, X. Duan, *Acc. Chem. Res.* **2015**, *48*, 1666.

[62] Z. Tan, *RSC Adv.* **2014**, *v. 4*, 8874.

[63] L. Liu, J. Zhai, C. Zhu, Y. Gao, Y. Wang, Y. Han, S. Dong, *Biosens. Bioelectron.* **2015**, *63*, 483.

[64] Q. Zhu, J. Bao, D. Huo, M. Yang, C. Hou, J. Guo, M. Chen, H. Fa, X. Luo, Y. Ma, *Sens. Actuators B Chem.* **2017**, *238*, 1316.

[65] Z. Tai, J. Yang, Y. Qi, X. Yan, Q. Xue, *RSC Adv.* **2013**, *3*, 12751.

[66] H. Bai, C. Li, X. Wang, G. Shi, *Chem. Commun.* **2010**, *46*, 2376.

[67] K. Sheng, Y. Xu, C. Li, G. Shi, *New Carbon Mater.* **2011**, *26*, 9.

[68] Z. Zhang, F. Xiao, Y. Guo, S. Wang, Y. Liu, *ACS Appl. Mater. Interfaces* **2013**, *5*, 2227.

[69] H. H. Bay, R. Vo, X. Dai, H.-H. Hsu, Z. Mo, S. Cao, W. Li, F. G. Omenetto, X. Jiang, *Nano Lett.* **2019**, *19*, 2620.

[70] S. Rafieian, H. Mirzadeh, H. Mahdavi, M. E. Masoumi, *Sci. Eng. Compos. Mater.* **2019**, *26*, 154.

[71] S. Iijima, *Nature* **1991**, *354*, 56.

[72] S. Iijima, T. Ichihashi, *Nature* **1993**, *363*, 603.

[73] J. Prasek, J. Drbohlavova, J. Chomoucka, J. Hubalek, O. Jasek, V. Adam, R. Kizek, *J. Mater. Chem.* **2011**, *21*, 15872.

[74] R. Smajda, J. C. Andresen, M. Duchamp, R. Meunier, S. Casimirius, K. Hernádi, L. Forró, A. Magrez, *Synthesis and mechanical properties of carbon nanotubes produced by the water assisted CVD process*, Vol. 246, John Wiley & Sons, Ltd, **2009**, 2457–2460.

[75] R. L. Vander Wal, G. M. Berger, T. M. Ticich, *Appl. Phys. A* **2003**, *77*, 885.

[76] C. Journet, W. K. Maser, P. Bernier, A. Loiseau, M. L. de la Chapelle, S. Lefrant, P. Deniard, R. Lee, J. E. Fischer, *Nature* **1997**, *388*, 756.

[77] M. J. Bronikowski, P. A. Willis, D. T. Colbert, K. A. Smith, R. E. Smalley, *J. Vac. Sci. Technol. Vac. Surf. Films* **2001**, *19*, 1800.

[78] A. Krishnan, E. Dujardin, T. W. Ebbesen, P. N. Yianilos, M. M. J. Treacy, *Phys. Rev. B* **1998**, *58*, 14013.

[79] R. H. Baughman, A. A. Zakhidov, W. A. de Heer, *Science* **2002**, *297*, 787.

[80] V. N. Popov, *Mater. Sci. Eng. R Rep.* **2004**, *43*, 61.

[81] A. Kavosi, S. Hosseini Ghale Noei, S. Madani, S. Khalighfard, S. Khodayari, H. Khodayari, M. Mirzaei, M. R. Kalhori, M. Yavarian, A. M. Alizadeh, M. Falahati, *Sci. Rep.* **2018**, *8*, 8375.

[82] Y. Zhu, W. Li, *Sci. China Ser. B Chem.* **2008**, *51*, 1021.

[83] V. Georgakilas, K. Kordatos, M. Prato, D. M. Guldi, M. Holzinger, A. Hirsch, *J. Am. Chem. Soc.* **2002**, *124*, 760.

[84] A. Hirsch, O. Vostrowsky, In *Functional Molecular Nanostructures: -/-* (Ed.: Schlüter, A. D.), Springer, Berlin, Heidelberg, **2005**, 193–237.

[85] M. Holzinger, O. Vostrowsky, A. Hirsch, F. Hennrich, M. Kappes, R. Weiss, F. Jellen, *Sidewall Functionalization of Carbon Nanotubes*, Vol. 40, John Wiley & Sons, Ltd, **2001**, 4002–4005.

[86] M. Shim, N. W. Shi Kam, R. J. Chen, Y. Li, H. Dai, *Nano Lett.* **2002**, *2*, 285.

[87] D. Tasis, N. Tagmatarchis, V. Georgakilas, M. Prato, *Soluble Carbon Nanotubes*, Vol. 9, John Wiley & Sons, Ltd, **2003**, 4000–4008.

[88] M. J. O'Connell, P. Boul, L. M. Ericson, C. Huffman, Y. Wang, E. Haroz, C. Kuper, J. Tour, K. D. Ausman, R. E. Smalley, *Chem. Phys. Lett.* **2001**, *342*, 265.

[89] A. K. Gaharwar, A. Patel, A. Dolatshahi-Pirouz, H. Zhang, K. Rangarajan, G. Iviglia, S.-R. Shin, M. A. Hussain, A. Khademhosseini, *Biomater. Sci.* **2015**, *3*, 46.

[90] X. Zhang, C. L. Pint, M. H. Lee, B. E. Schubert, A. Jamshidi, K. Takei, H. Ko, A. Gillies, R. Bardhan, J. J. Urban, M. Wu, R. Fearing, A. Javey, *Nano Lett.* **2011**, *11*, 3239.

[91] X. Tong, J. Zheng, Y. Lu, Z. Zhang, H. Cheng, *Mater. Lett.* **2007**, *61*, 1704.

[92] T. Tungkavet, N. Seetapan, D. Pattavarakorn, A. Sirivat, *Mater. Sci. Eng. C* **2015**, *46*, 281.

[93] N. S. Satarkar, D. Johnson, B. Marrs, R. Andrews, C. Poh, B. Gharaibeh, K. Saito, K. W. Anderson, J. Z. Hilt, *Hydrogel-MWCNT nanocomposites: Synthesis, characterization, and heating with radiofrequency fields*, Vol. 117, John Wiley & Sons, Ltd, **2010**, 1813–1819.

[94] H. Liu, M. Liu, L. Zhang, L. Ma, J. Chen, Y. Wang, *React. Funct. Polym.* **2010**, *70*, 294.

[95] Z. Liu, A. Lu, Z. Yang, Y. Luo, *Macromol. Res.* **2013**, *21*, 376.

[96] E. Lee, J. Park, S. G. Im, C. Song, *Polym. Chem.* **2012**, *3*, 2451.

[97] J. Cui, M. Björnmalm, K. Liang, C. Xu, J. Best, X. Zhang, F. Caruso, *Adv. Mater.* **2014**, *26*.

[98] L. Li, J. Meng, M. Zhang, T. Liu, C. Zhang, *Chem. Commun.* **2022**, *58*, 185.

[99] L. Wang, T. Xu, X. Zhang, *TrAC Trends Anal. Chem.* **2021**, *134*, 116130.

[100] R. A. Green, R. T. Hassarati, J. A. Goding, S. Baek, N. H. Lovell, P. J. Martens, L. A. Poole-Warren, *Macromol. Biosci.* **2012**, *12*, 494.

[101] C. R. Martin, *Acc. Chem. Res.* **1995**, *28*, 61.

[102] Y. Wang, Y. Shi, L. Pan, Y. Ding, Y. Zhao, Y. Li, Y. Shi, G. Yu, *Nano Lett.* **2015**, *15*, 7736.

[103] B. C. Kim, G. M. Spinks, G. G. Wallace, R. John, *Polymer* **2000**, *41*, 1783.

[104] L. Pan, G. Yu, D. Zhai, H. R. Lee, W. Zhao, N. Liu, H. Wang, B. C.-K. Tee, Y. Shi, Y. Cui, Z. Bao, *Proc. Natl. Acad. Sci.* **2012**, *109*, 9287.

[105] Q. Rong, H. Han, F. Feng, Z. Ma, *Sci. Rep.* **2015**, *5*, 11440.

[106] Y. Shi, C. Ma, L. Peng, G. Yu, *Conductive "Smart" Hybrid Hydrogels with PNIPAM and Nanostructured Conductive Polymers*, Vol. 25, John Wiley & Sons, Ltd, **2015**, 1219–1225.

[107] L. Li, Y. Wang, L. Pan, Y. Shi, W. Cheng, Y. Shi, G. Yu, *Nano Lett.* **2015**, *15*, 1146.

[108] P. Humpolíček, K. A. Radaszkiewicz, Z. Capáková, J. Pacherník, P. Bober, V. Kašpárková, P. Rejmontová, M. Lehocký, P. Ponížil, J. Stejskal, *Sci. Rep.* **2018**, *8*, 135.

[109] X.-W. Liu, Y.-X. Huang, X.-F. Sun, G.-P. Sheng, F. Zhao, S.-G. Wang, H.-Q. Yu, *ACS Appl. Mater. Interfaces* **2014**, *6*, 8158.

[110] B. Chu, D. Zhang, P. J. Paukstelis, *Nucleic Acids Res.* **2019**, *47*, 11921.

[111] H.-Q. Chen, W. Yang, H. Zuo, H.-W. He, Y.-J. Wang, *J. Anal. Test.* **2021**, *5*, 155.

[112] W. Xu, Y. Huang, H. Zhao, P. Li, G. Liu, J. Li, C. Zhu, L. Tian, *DNA Hydrogel with Tunable pH-Responsive Properties Produced by Rolling Circle Amplification*, Vol. 23, John Wiley & Sons, Ltd, **2017**, 18276–18281.

[113] Y. Xing, E. Cheng, Y. Yang, P. Chen, T. Zhang, Y. Sun, Z. Yang, D. Liu, *Self-Assembled DNA Hydrogels with Designable Thermal and Enzymatic Responsiveness*, Vol. 23, John Wiley & Sons, Ltd, **2011**, 1117–1121.

[114] S. H. Um, J. B. Lee, N. Park, S. Y. Kwon, C. C. Umbach, D. Luo, *Nat. Mater.* **2006**, *5*, 797.

[115] H. Jiang, V. Pan, S. Vivek, E. R. Weeks, Y. Ke, *Programmable DNA Hydrogels Assembled from Multidomain DNA Strands*, Vol. 17, John Wiley & Sons, Ltd, **2016**, pp. 1156–1162.

[116] E. Cheng, Y. Xing, P. Chen, Y. Yang, Y. Sun, D. Zhou, L. Xu, Q. Fan, D. Liu, *A pH-Triggered, Fast-Responding DNA Hydrogel*, Vol. 48, John Wiley & Sons, Ltd, **2009**, 7660–7663.

[117] H. Kang, H. Liu, X. Zhang, J. Yan, Z. Zhu, L. Peng, H. Yang, Y. Kim, W. Tan, *Langmuir* **2011**, *27*, 399.

[118] W. Guo, X.-J. Qi, R. Orbach, C.-H. Lu, L. Freage, I. Mironi-Harpaz, D. Seliktar, H.-H. Yang, I. Willner, *Chem. Commun.* **2014**, *50*, 4065.

[119] Y. Dong, Z. Yang, D. Liu, *Acc. Chem. Res.* **2014**, *47*, 1853.

[120] F. Wang, X. Liu, I. Willner, *DNA Switches: From Principles to Applications*, Vol. 54, John Wiley & Sons, Ltd, **2015**, pp. 1098–1129.

[121] C.-H. Lu, X.-J. Qi, R. Orbach, H.-H. Yang, I. Mironi-Harpaz, D. Seliktar, I. Willner, *Nano Lett.* **2013**, *13*, 1298.

[122] J. S. Kahn, Y. Hu, I. Willner, *Acc. Chem. Res.* **2017**, *50*, 680.

[123] H. Liu, T. Cao, Y. Xu, Y. Dong, D. Liu, *Int. J. Mol. Sci.* **2018**, *19*, 1633.

[124] J. Li, C. Zheng, S. Cansiz, C. Wu, J. Xu, C. Cui, Y. Liu, W. Hou, Y. Wang, L. Zhang, I. Teng, H.-H. Yang, W. Tan, *J. Am. Chem. Soc.* **2015**, *137*, 1412.

[125] Y. Lin, X. Wang, Y. Sun, Y. Dai, W. Sun, X. Zhu, H. Liu, R. Han, D. Gao, C. Luo, *Sens. Actuators B Chem.* **2019**, *289*, 56.

[126] W. Cai, S. Xie, J. Zhang, D. Tang, Y. Tang, *Biosens. Bioelectron.* **2017**, *98*, 466.

[127] Y. He, X. Yang, R. Yuan, Y. Chai, *J. Mater. Chem. B* **2019**, *7*, 2643.

[128] X. Mao, D. Mao, T. Chen, M. Jalalah, M. S. Al-Assiri, F. A. Harraz, X. Zhu, G. Li, *ACS Appl. Mater. Interfaces* **2020**, *12*, 36851.

[129] A. Baeissa, N. Dave, B. D. Smith, J. Liu, *ACS Appl. Mater. Interfaces* **2010**, *2*, 3594.

[130] X. Mao, S. Pan, D. Zhou, X. He, Y. Zhang, *Sens. Actuators B Chem.* **2019**, *285*, 385.

[131] H. Zhao, G. Jiang, J. Weng, Q. Ma, H. Zhang, Y. Ito, M. Liu, *J. Mater. Chem. B* **2016**, *4*, 4648.

[132] P. A. Korevaar, C. N. Kaplan, A. Grinthal, R. M. Rust, J. Aizenberg, *Nat. Commun.* **2020**, *11*, 386.

[133] M. Radecki, J. Spěváček, A. Zhigunov, Z. Sedláková, L. Hanyková, *Eur. Polym. J.* **2015**, *68*, 68.

[134] S. Cai, Z. Suo, *J. Mech. Phys. Solids* **2011**, *59*, 2259.

[135] N. Zhang, S. Zheng, Z. Pan, Z. Liu, *Polymers* **2018**, *10*, 358.

[136] S. I. Kang, Y. H. Bae, *Macromolecules* **2001**, *34*, 8173.

[137] T. Wu, H. Li, *Phys. Chem. Chem. Phys.* **2017**, *19*, 21012.

[138] D. Yang, A. Wang, J.-H. Chen, X.-C. Yu, C. Lan, Y. Ji, Y.-F. Xiao, *Photonics Res.* **2020**, *8*, 497.

[139] C. Norioka, K. Okita, M. Mukada, A. Kawamura, T. Miyata, *Polym. Chem.* **2017**, *8*, 6378.

[140] S. Bennour, F. Louzri, *Adv. Chem.* **2014**, *2014*, 147398.

[141] A. S. Kipcak, O. Ismail, I. Doymaz, S. Piskin, *J. Chem.* **2014**, *2014*, 281063.

[142] M. Betz, J. Hörmansperger, T. Fuchs, U. Kulozik, *Soft Matter* **2012**, *8*, 2477.

[143] H. Kojima, *Polym. J.* **2018**, *50*, 411.

[144] A. Ehrenhofer, M. Elstner, T. Wallmersperger, *Sens. Actuators B Chem.* **2018**, *255*, 1343.

[145] E. Karadağ, D. Saraydin, S. Çetinkaya, O. Güven, *Biomaterials* **1996**, *17*, 67.

[146] S. Ahadian, R. B. Sadeghian, S. Salehi, S. Ostrovidov, H. Bae, M. Ramalingam, A. Khademhosseini, *Bioconjug. Chem.* **2015**, *26*, 1984.

[147] M. Dessi, A. Borzacchiello, T. H. A. Mohamed, W. I. Abdel-Fattah, L. Ambrosio, *Novel biomimetic thermosensitive β-tricalcium phosphate/chitosan-based hydrogels for bone tissue engineering*, Vol. 101, John Wiley & Sons, Ltd, **2013**, 2984–2993.

[148] M. E. Furth, A. Atala, M. E. Van Dyke, *Festschr. Honouring Profr. David F Williams* **2007**, *28*, 5068.

[149] A. S. Gobin, J. L. West, *Effects of Epidermal Growth Factor on Fibroblast Migration through Biomimetic Hydrogels*, Vol. 19, American Chemical Society (ACS), **2003**,1781–1785.

[150] M. Gonen-Wadmany, L. Oss-Ronen, D. Seliktar, *Biomaterials* **2007**, *28*, 3876.

[151] J. Lu, X. Wang, In *Biomimetic Medical Materials: From Nanotechnology to 3D Bioprinting* (Ed.: Noh, I.), Springer, Singapore, **2018**, pp. 297–312.

[152] S. Mantha, S. Pillai, P. Khayambashi, A. Upadhyay, Y. Zhang, O. Tao, H. M. Pham, S. D. Tran, *Mater. Basel Switz.* **2019**, *12*, 3323.

[153] J. Patterson, M. M. Martino, J. A. Hubbell, *Mater. Today* **2010**, *13*, 14.

[154] J. Sawayama, T. Okitsu, A. Nakamata, Y. Kawahara, S. Takeuchi, *iScience* **2020**, *23*, 101243.

[155] B. Linke, W. Kerner, M. Kiwit, M. Pishko, A. Heller, *Biosens. Bioelectron.* **1994**, *9*, 151.

[156] N. Farhoudi, L. B. Laurentius, J. J. Magda, C. F. Reiche, F. Solzbacher, *ACS Sens.* **2021**, *6*, 3587.

[157] I. Ali, L. A. Shah, *Polym. Bull.* **2020**.

[158] T. V. Budtova, V. P. Budtov, P. Navard, S. Y. Frenkel, *Rheological properties of highly swollen hydrogel suspensions*, Vol. 52, John Wiley & Sons, Ltd, **1994**, 721–726.

[159] F. Cuomo, M. Cofelice, F. Lopez, *Polymers* **2019**, *11*, 259.

[160] S. R. Derkach, N. G. Voron'ko, N. I. Sokolan, *J. Dispers. Sci. Technol.* **2017**, *38*, 1427.

[161] K. Ghosh, X. Z. Shu, R. Mou, J. Lombardi, G. D. Prestwich, M. H. Rafailovich, R. A. F. Clark, *Biomacromolecules* **2005**, *6*, 2857.

[162] E. Gicquel, C. Martin, Q. Gauthier, J. Engström, C. Abbattista, A. Carlmark, E. D. Cranston, B. Jean, J. Bras, *Biomacromolecules* **2019**, *20*, 2545.

[163] H. Jiang, W. Su, P. T. Mather, T. J. Bunning, *Polymer* **1999**, *40*, 4593.

[164] R. Kocen, M. Gasik, A. Gantar, S. Novak, *Biomed. Mater.* **2017**, *12*, 025004.

[165] Z. Xing, A. Caciagli, T. Cao, I. Stoev, M. Zupkauskas, T. O'Neill, T. Wenzel, R. Lamboll, D. Liu, E. Eiser, *Proc. Natl. Acad. Sci.* **2018**, *115*, 8137.

[166] C. Yan, D. J. Pochan, *Chem. Soc. Rev.* **2010**, *39*, 3528.

[167] R. A. Green, S. Baek, L. A. Poole-Warren, P. J. Martens, *Sci. Technol. Adv. Mater.* **2010**, *11*, 014107.

[168] S. Dolai, H. Leu, J. Magda, M. Tabib-Azar, In *2018 IEEE SENSORS*, **2018**, pp. 1–4.

[169] L. Fillaud, T. Petenzi, J. Pallu, B. Piro, G. Mattana, V. Noel, *Langmuir ACS J. Surf. Colloids* **2018**, *34*, 3686.

[170] Y. J. Jo, K. Y. Kwon, Z. U. Khan, X. Crispin, T. Kim, *ACS Appl. Mater. Interfaces* **2018**, *10*, 39083.

[171] D. Lai, E. Li, Y. Yan, Y. Liu, J. Zhong, D. Lv, Y. Ke, H. Chen, T. Guo, *Org. Electron.* **2019**, *75*, 105409.

[172] E. Lai, X. Yue, W. Ning, J. Huang, X. Ling, H. Lin, *Front. Chem.* **2019**, *7*.

[173] H. Li, T. Lv, H. Sun, G. Qian, N. Li, Y. Yao, T. Chen, *Nat. Commun.* **2019**, *10*, 536.

[174] B.-S. Yin, S.-W. Zhang, K. Ke, Z.-B. Wang, *J. Alloys Compd.* **2019**, *805*, 1044.

[175] S. J. Little, S. F. Ralph, N. Mano, J. Chen, G. G. Wallace, *Chem. Commun.* **2011**, *47*, 8886.

[176] L. He, D. Lin, Y. Wang, Y. Xiao, J. Che, *Colloids Surf. B Biointerfaces* **2011**, *87*, 273.

[177] T. Kajisa, T. Sakata, *Sci. Technol. Adv. Mater.* **2017**, *18*, 26.

[178] A. P. Mártire, G. M. Segovia, O. Azzaroni, M. Rafti, W. Marmisollé, *Mol. Syst. Des. Eng.* **2019**, *4*, 893.

[179] A. A. Homaei, R. Sariri, F. Vianello, R. Stevanato, *J. Chem. Biol.* **2013**, *6*, 185.

[180] N. R. Mohamad, N. H. C. Marzuki, N. A. Buang, F. Huyop, R. A. Wahab, *Biotechnol. Biotechnol. Equip.* **2015**, *29*, 205.

[181] D. Magnin, S. Dumitriu, E. Chornet, *J. Bioact. Compat. Polym.* **2003**, *18*, 355.

[182] D. Magnin, S. Dumitriu, P. Magny, E. Chornet, *Lipase Immobilization into Porous Chitoxan Beads: Activities in Aqueous and Organic Media and Lipase Localization*, Vol. 17, American Chemical Society (ACS), **2001**, 734–737.

[183] A. K. Dwamena, S. H. Woo, C. S. Kim, *Biotechnol. Lett.* **2020**, *42*, 845.

[184] M. Piao, D. Zou, Y. Yang, X. Ren, C. Qin, Y. Piao, *Mater. Basel Switz.* **2019**, *12*, 704.

[185] J. Y. C. Lim, S. S. Goh, X. J. Loh, *ACS Mater. Lett.* **2020**, *2*, 918.

[186] D. Zhai, B. Liu, Y. Shi, L. Pan, Y. Wang, W. Li, R. Zhang, G. Yu, *ACS Nano* **2013**, *7*, 3540.

[187] Y. Kim, H. Namgung, T. S. Lee, *Polym. Chem.* **2016**, *7*, 6655.

[188] J. H. Kim, S. Y. Lim, D. H. Nam, J. Ryu, S. H. Ku, C. B. Park, *Biosens. Bioelectron.* **2011**, *26*, 1860.

[189] J. Yuan, D. Wen, N. Gaponik, A. Eychmüller, *Enzyme-Encapsulating Quantum Dot Hydrogels and Xerogels as Biosensors: Multifunctional Platforms for Both Biocatalysis and Fluorescent Probing*, Vol. 52, John Wiley & Sons, Ltd, **2013**, 976–979.

[190] C. A. P. Quinn, R. E. Connor, A. Heller, *Biomaterials* **1997**, *18*, 1665.

[191] A. L. Crumbliss, J. G. Stonehuerner, R. W. Henkens, J. Zhao, J. P. O'Daly, *Biosens. Bioelectron.* **1993**, *8*, 331.

[192] J. Erfkamp, M. Guenther, G. Gerlach, *Sensors* **2019**, *19*, 2858.

[193] Y. Huang, Y. Ding, T. Li, M. Yang, *Anal. Methods* **2015**, *7*, 411.

[194] A. Pollap, J. Kochana, *Biosensors* **2019**, *9*, 61.

[195] Z. Tang, Y. Fu, Z. Ma, *Biosens. Bioelectron.* **2017**, *91*, 299.

[196] H. Wang, H. Han, Z. Ma, *Bioelectrochemistry* **2017**, *114*, 48.

[197] H. Wang, Z. Ma, *Sens. Actuators B Chem.* **2018**, *254*, 642.

[198] L. Zhao, S. Yin, Z. Ma, *ACS Sens.* **2019**, *4*, 450.

[199] W. Li, Z. Ma, *Sens. Actuators B Chem.* **2017**, *248*, 545.

[200] X. Zhang, S. Wang, M. Hu, Y. Xiao, *Biosens. Bioelectron.* **2006**, *21*, 2180.

[201] F. Ma, C.-W. Yuan, J.-N. Liu, J.-H. Cao, D.-Y. Wu, *ACS Appl. Mater. Interfaces* **2019**, *11*, 19902.

[202] L. Shen, P. He, *Electrochem. Commun.* **2007**, *9*, 657.

[203] S. L. Lim, C.-W. Ooi, W. S. Tan, E.-S. Chan, K. L. Ho, B. T. Tey, *Sens. Actuators B Chem.* **2017**, *252*, 409.

[204] M. Frasconi, M. Mazzarino, F. Botrè, F. Mazzei, *Anal. Bioanal. Chem.* **2009**, *394*, 2151.

[205] Y. Hou, T. Li, H. Huang, H. Quan, X. Miao, M. Yang, *Sens. Actuators B Chem.* **2013**, *182*, 605.

[206] H. Inan, M. Poyraz, F. Inci, M. A. Lifson, M. Baday, B. T. Cunningham, U. Demirci, *Chem. Soc. Rev.* **2017**, *46*, 366.

[207] J. H. Holtz, S. A. Asher, *Nature* **1997**, *389*, 829.

[208] J. Qin, X. Li, L. Cao, S. Du, W. Wang, S. Q. Yao, *J. Am. Chem. Soc.* **2020**, *142*, 417.

[209] C.-H. Lu, W. Guo, Y. Hu, X.-J. Qi, I. Willner, *J. Am. Chem. Soc.* **2015**, *137*, 15723.

[210] Y. Di, P. Wang, C. Li, S. Xu, Q. Tian, T. Wu, Y. Tian, L. Gao, *Front. Med.* **2020**, *7*, 456.

[211] Z. Zhu, C. Wu, H. Liu, Y. Zou, X. Zhang, H. Kang, C. J. Yang, W. Tan, *An Aptamer Cross-Linked Hydrogel as a Colorimetric Platform for Visual Detection*, Vol. 49, John Wiley & Sons, Ltd, **2010**, 1052–1056.

[212] I. Y. Jung, J. S. Kim, B. R. Choi, K. Lee, H. Lee, *Hydrogel Based Biosensors for In Vitro Diagnostics of Biochemicals, Proteins, and Genes*, Vol. 6, John Wiley & Sons, Ltd, **2017**.

[213] Y. Helwa, N. Dave, R. Froidevaux, A. Samadi, J. Liu, *ACS Appl. Mater. Interfaces* **2012**, *4*, 2228.

[214] W. Bai, D. A. Spivak, *A Double-Imprinted Diffraction-Grating Sensor Based on a Virus-Responsive Super-Aptamer Hydrogel Derived from an Impure Extract*, Vol. 53, John Wiley & Sons, Ltd, **2014**, 2095–2098.

[215] R. Wang, Y. Li, *Biosens. Bioelectron.* **2013**, *42*, 148.

[216] A. K. H. Cheng, D. Sen, H.-Z. Yu, *Bioelectrochemistry* **2009**, *77*, 1.

[217] X. Gao, L. Qi, K. Liu, C. Meng, Y. Li, H.-Z. Yu, *Anal. Chem.* **2020**, *92*, 6229.

[218] Y. He, X. Yang, R. Yuan, Y. Chai, *Anal. Chem.* **2017**, *89*, 8538.

[219] W. Choi, S. Y. Yeom, J. Kim, S. Jung, S. Jung, T. S. Shim, S. K. Kim, J. Y. Kang, S. H. Lee, I.-J. Cho, J. Choi, N. Choi, *Biosens. Bioelectron.* **2018**, *101*, 235.

[220] S. C. Chapin, P. S. Doyle, *Anal. Chem.* **2011**, *83*, 7179.

[221] E. Gil-Santos, J. J. Ruz, O. Malvar, I. Favero, A. Lemaître, Priscila. M. Kosaka, S. García-López, M. Calleja, J. Tamayo, *Nat. Nanotechnol.* **2020**, *15*, 469.

[222] S.-H. Lee, S. Shin, Y. Roh, S. J. Oh, S. H. Lee, H. S. Song, Y.-S. Ryu, Y. K. Kim, M. Seo, *Biosens. Bioelectron.* **2020**, *170*, 112663.

[223] J. Zhou, X. Zhao, G. Huang, X. Yang, Y. Zhang, X. Zhan, H. Tian, Y. Xiong, Y. Wang, W. Fu, *ACS Sens.* **2021**, *6*, 1884.

[224] M. K. Masud, Nanoarchitectured point-of-care detection system for clinically relevant biomarkers, Doctoral Dissertation, University of Queensland, **2020**.

[225] X. Han, J. Wang, Y. Sun, *Biomark. Hum. Dis. Transl. Med.* **2017**, *15*, 59.

[226] H. Jin, Y. Ma, Q. Shen, X. Wang, *Circulating Methylated DNA as Biomarkers for Cancer Detection*, IntechOpen, **2012**.

[227] Z. Dong, X. Xue, H. Liang, J. Guan, L. Chang, *Anal. Chem.* **2021**, *93*, 1855.

[228] Y. Zhao, X. Zhao, B. Tang, W. Xu, J. Li, J. Hu, Z. Gu, *Adv. Funct. Mater.* **2010**, *20*, 976.

[229] X. Hua, X. Zhou, S. Guo, T. Zheng, R. Yuan, W. Xu, *Microchim. Acta* **2019**, *186*, 158.

[230] X. Gao, X. Li, X. Sun, J. Zhang, Y. Zhao, X. Liu, F. Li, *Anal. Chem.* **2020**, *92*, 4592.

[231] D. Al Sulaiman, J. Y. H. Chang, N. R. Bennett, H. Topouzi, C. A. Higgins, D. J. Irvine, S. Ladame, *ACS Nano* **2019**, *13*, 9620.

[232] Cancer Genome Atlas Network, *Nature* **2012**, *490*, 61.

[233] J.-H. Hwang, J. Voortman, E. Giovannetti, S. M. Steinberg, L. G. Leon, Y.-T. Kim, N. Funel, J. K. Park, M. A. Kim, G. H. Kang, S.-W. Kim, M. Del Chiaro, G. J. Peters, G. Giaccone, *PloS One* **2010**, *5*, e10630.

[234] A. Cordeiro, A. Navarro, A. Gaya, M. Díaz-Beyá, B. Gonzalez-Farré, J. J. Castellano, D. Fuster, C. Martínez, A. Martínez, M. Monzó, *Oncotarget* **2016**, *7*, 46002.

[235] J. Liao, L. Yu, Y. Mei, M. Guarnera, J. Shen, R. Li, Z. Liu, F. Jiang, *Mol. Cancer* **2010**, *9*, 198.

[236] Y. Si, L. Xu, N. Wang, J. Zheng, R. Yang, J. Li, *Anal. Chem.* **2020**, *92*, 2649.

[237] S. Deng, J. Yan, F. Wang, Y. Su, X. Zhang, Q. Li, G. Liu, C. Fan, H. Pei, Y. Wan, *Biosens. Bioelectron.* **2019**, *137*, 263.

[238] D. Al Sulaiman, S. J. Shapiro, J. Gomez-Marquez, P. S. Doyle, *ACS Sens.* **2021**, *6*, 203.

[239] S. Mohammadi, S. Mohammadi, A. Salimi, *Talanta* **2021**, *224*, 121895.

[240] B. Salahuddin, M. K. Masud, S. Aziz, C.-H. Liu, N. Amiralian, A. Ashok, S. M. A. Hossain, H. Park, M. A. Wahab, M. A. Amin, M. A. Chari, A. E. Rowan, Y. Yamauchi, Md. S. A. Hossain, Y. V. Kaneti, *Bull. Chem. Soc. Jpn.* **2022**, *95*, 198.

[241] M. K. Masud, S. Yadav, Md. N. Islam, N.-T. Nguyen, C. Salomon, R. Kline, H. R. Alamri, Z. A. Alothman, Y. Yamauchi, Md. S. A. Hossain, M. J. A. Shiddiky, *Anal. Chem.* **2017**, *89*, 11005.

[242] M. K. Masud, J. Kim, Md. M. Billah, K. Wood, M. J. A. Shiddiky, N.-T. Nguyen, R. K. Parsapur, Y. V. Kaneti, A. A. Alshehri, Y. G. Alghamidi, K. A. Alzahrani, M. Adharvanachari, P. Selvam, Md. S. A. Hossain, Y. Yamauchi, *J. Mater. Chem. B* **2019**, *7*, 5412.

[243] S. Tanaka, M. K. Masud, Y. V. Kaneti, M. J. A. Shiddiky, A. Fatehmulla, A. M. Aldhafiri, W. A. Farooq, Y. Bando, Md. S. A. Hossain, Y. Yamauchi, *ChemNanoMat* **2019**, *5*, 506.

[244] S. M. George, S. Tandon, B. Kandasubramanian, *ACS Omega* **2020**, *5*, 2060.

[245] N. Pourreza, M. Ghomi, *Anal. Chim. Acta* **2019**, *1079*, 180.

[246] H. Mitomo, K. Horie, Y. Matsuo, K. Niikura, T. Tani, M. Naya, K. Ijiro, *Adv. Opt. Mater.* **2016**, *4*, 259.

[247] F. Alimirah, J. Chen, Z. Basrawala, H. Xin, D. Choubey, *FEBS Lett.* **2006**, *580*, 2294.

[248] T. A. Ince, A. D. Sousa, M. A. Jones, J. C. Harrell, E. S. Agoston, M. Krohn, L. M. Selfors, W. Liu, K. Chen, M. Yong, P. Buchwald, B. Wang, K. S. Hale, E. Cohick, P. Sergent, A. Witt, Z. Kozhekbaeva, S. Gao, A. T. Agoston, M. A. Merritt, R. Foster, B. R. Rueda, C. P. Crum, J. S. Brugge, G. B. Mills, *Nat. Commun.* **2015**, *6*, 7419.

[249] C. K. Osborne, K. Hobbs, J. M. Trent, *Breast Cancer Res. Treat.* **1987**, *9*, 111.

[250] B. Purohit, A. Kumar, K. Mahato, S. Roy, P. Chandra, In *Nanotechnology in Modern Animal Biotechnology* (Eds.: Maurya, P. K.; Singh, S.), Elsevier, **2019**, 133–147.

[251] D. Ye, M. Li, T. Zhai, P. Song, L. Song, H. Wang, X. Mao, F. Wang, X. Zhang, Z. Ge, J. Shi, L. Wang, C. Fan, Q. Li, X. Zuo, *Nat. Protoc.* **2020**, *15*, 2163.

[252] C. Hao, L. Ding, X. Zhang, H. Ju, *Anal. Chem.* **2007**, *79*, 4442.

[253] N. Massad-Ivanir, G. Shtenberg, T. Zeidman, E. Segal, *Adv. Funct. Mater.* **2010**, *20*, 2269.

[254] G. Valenti, S. Scarabino, B. Goudeau, A. Lesch, M. Jović, E. Villani, M. Sentic, S. Rapino, S. Arbault, F. Paolucci, N. Sojic, *J. Am. Chem. Soc.* **2017**, *139*, 16830.

[255] G. Liu, C. Ma, B.-K. Jin, Z. Chen, F.-L. Cheng, J.-J. Zhu, *Anal. Chem.* **2019**, *91*, 3021.

[256] C. Ding, Y. Li, L. Wang, X. Luo, *Anal. Chem.* **2019**, *91*, 983.

[257] G. Liu, Z. Chen, B.-K. Jin, L.-P. Jiang, *Analyst* **2021**, *146*, 1835.

[258] S. Sharma, M. K. Masud, Y. V. Kaneti, P. Rewatkar, A. Koradia, Md. S. A. Hossain, Y. Yamauchi, A. Popat, C. Salomon, *Small* **2021**, 2102220.

[259] K. Boriachek, M. K. Masud, C. Palma, H.-P. Phan, Y. Yamauchi, Md. S. A. Hossain, N.-T. Nguyen, C. Salomon, M. J. A. Shiddiky, *Anal. Chem.* **2019**, *91*, 3827.

[260] J. Dai, Y. Su, S. Zhong, L. Cong, B. Liu, J. Yang, Y. Tao, Z. He, C. Chen, Y. Jiang, *Signal Transduct. Target. Ther.* **2020**, *5*, 145.

[261] V. I. Butvilovskaya, A. A. Tikhonov, E. N. Savvateeva, A. A. Ragimov, E. L. Salimov, S. A. Voloshin, D. V. Sidorov, M. A. Chernichenko, A. P. Polyakov, M. M. Filushin, M. V. Tsybulskaya, A. Yu. Rubina, *Mol. Biol.* **2017**, *51*, 712.

[262] W. Chen, J. Li, X. Wei, Y. Fan, H. Qian, S. Li, Y. Xiang, S. Ding, *Microchim. Acta* **2020**, *187*, 590.

[263] Q. Jiang, Y. Liu, L. Wang, G. B. Adkins, W. Zhong, *Anal. Chem.* **2019**, *91*, 15951.

[264] X. Mao, S. Pan, D. Zhou, X. He, Y. Zhang, *Sens. Actuators B Chem.* **2019**, *285*, 385.

[265] X. Hua, X. Zhou, S. Guo, T. Zheng, R. Yuan, W. Xu, *Microchim. Acta* **2019**, *186*, 158.

[266] L. Yang, H. Wang, H. Lü, N. Hui, *Anal. Chim. Acta* **2020**, *1124*, 104.

[267] Y. Si, L. Xu, N. Wang, J. Zheng, R. Yang, J. Li, *Anal. Chem.* **2020**, *92*, 2649.

[268] S. Mohammadi, S. Mohammadi, A. Salimi, *Talanta* **2021**, *224*, 121895.

[269] S. Deng, J. Yan, F. Wang, Y. Su, X. Zhang, Q. Li, G. Liu, C. Fan, H. Pei, Y. Wan, *Biosens. Bioelectron.* **2019**, *137*, 263.

[270] D. Al Sulaiman, S. J. Shapiro, J. Gomez-Marquez, P. S. Doyle, *ACS Sens.* **2021**, *6*, 203.

[271] N. Pourreza, M. Ghomi, *Anal. Chim. Acta* **2019**, *1079*, 180.

[272] J. Ji, W. Lu, Y. Zhu, H. Jin, Y. Yao, H. Zhang, Y. Zhao, *ACS Sens.* **2019**, *4*, 1384.

[273] D. Ye, M. Li, T. Zhai, P. Song, L. Song, H. Wang, X. Mao, F. Wang, X. Zhang, Z. Ge, J. Shi, L. Wang, C. Fan, Q. Li, X. Zuo, *Nat. Protoc.* **2020**, *15*, 2163.

[274] W. Chen, J. Li, X. Wei, Y. Fan, H. Qian, S. Li, Y. Xiang, S. Ding, *Microchim. Acta* **2020**, *187*, 590.

Figures

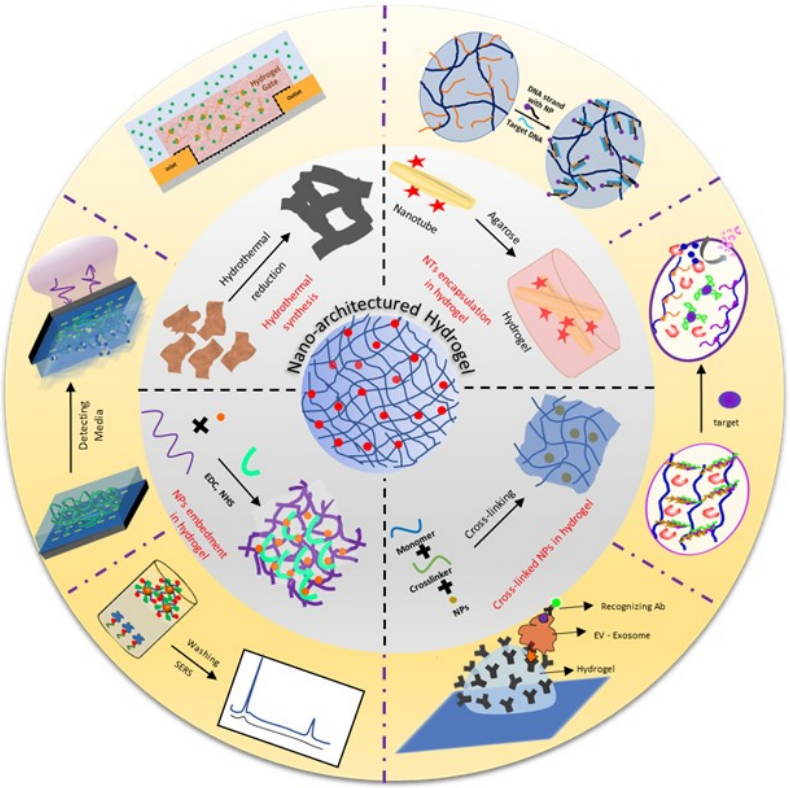

Scheme 1. Hydrogel nanoarchitectonics combines nanostructures with a 3D hydrogel to produce sophisticated, physically and chemically regulated, and tailored soft structures with synergistic properties for improved biocompatibility, biomolecule immobilization, and robust and sensitive biosensor design. Different techniques, including crosslinking, encapsulation, and hydrothermal conversion, can be used to integrate nanostructures with hydrogel. The potential for building specific biosensors for nucleic acid (DNA and RNA markers), protein, cells, and extracellular vesicles is enormous with these nanostructured hydrogels.

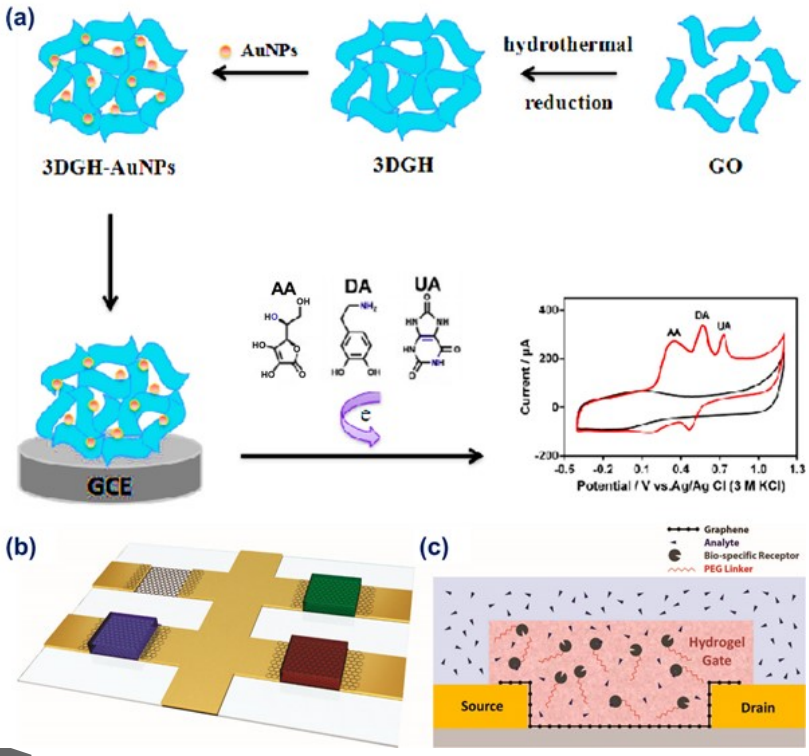

Figure 1. (a) Schematic representation for the preparation to quantification of ascorbic acid, dopamine and uric acid using 3D graphene hydrogel-gold nanostructure modified-GCE. Reproduced with permission.[64] Copyright 2016, Elsevier. (b) Graphene FET device arrays with independently decorated biologically encoded hydrogel, and (c) PEGylated receptors enclosed on graphene FET channels. Reproduced with permission.[69] Copyright 2019, American Chemical Society.

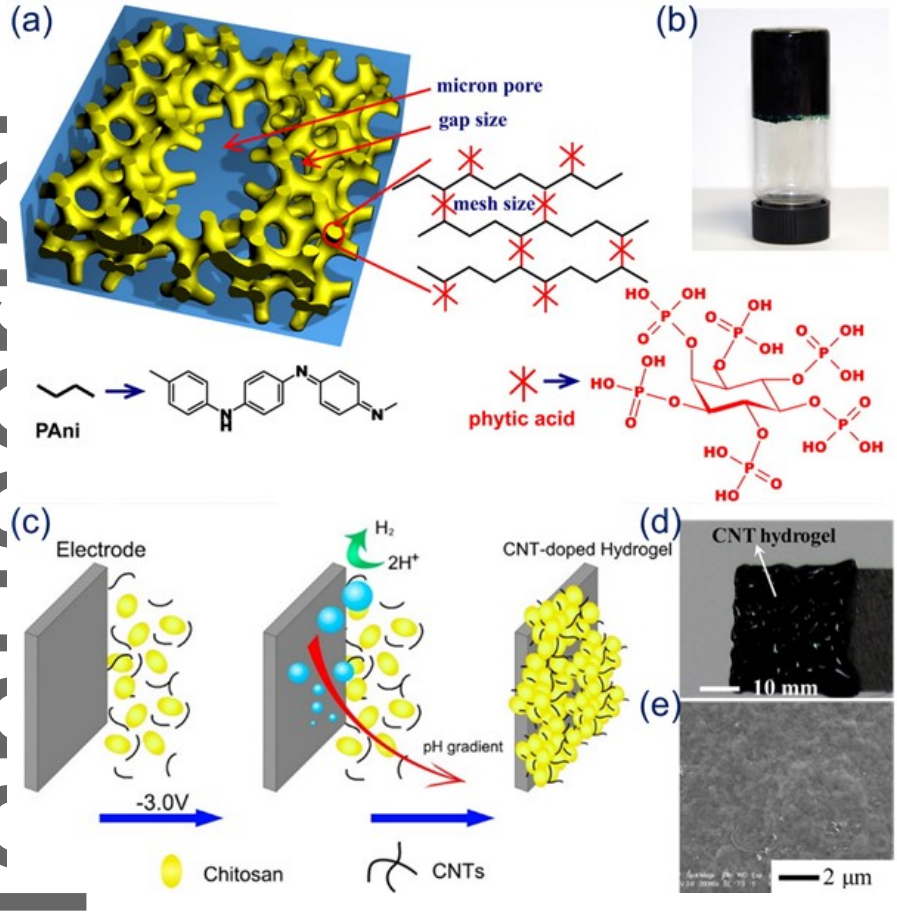

Figure 2. (a) Schematic representation of 3D microporous PAni hydrogel network. (b) PAni hydrogel inside a glass. Reproduced with permission.[104] Copyright 2012, Proceedings of National Academy of Sciences. (c) Fabrication of self-assembled CNT-hydrogel onto a carbon paper electrode through the simultaneous electrodeposition of both CNT and chitosan. (d) CNT hydrogel fabricated on carbon paper; and (e) SEM image of CNT hydrogel-modified paper. Reproduced with permission.[109] Copyright 2012, American Chemical Society.

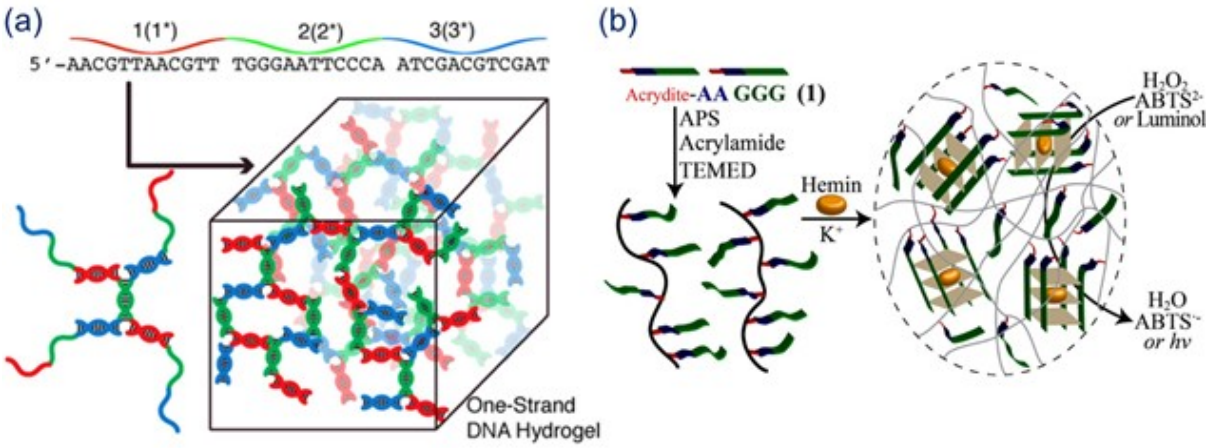

Figure 3. (a) Self-assembled one strand DNA hydrogel formation. Reproduced with permission.[115] Copyright 2016, Wiley-VCH. (b) Formation of K^+ induced hemin/acrylamide/G-quadruplex hydrogel. Reproduced with permission.[121] Copyright 2013, American Chemical Society.

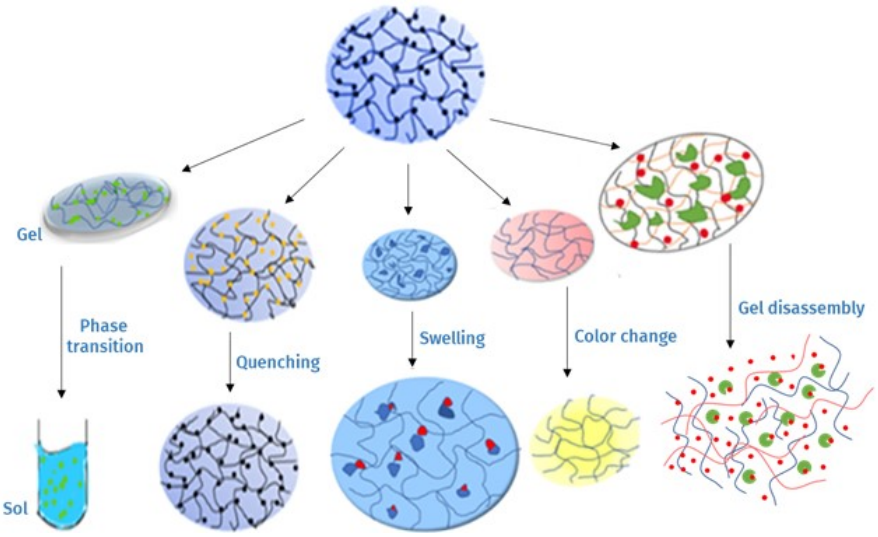

Figure 4. Schematic illustration of the mechanism of hydrogel biosensing. Hydrogel matrix can be modified purposefully for detecting the analyte of interest. In the presence of analyte, tailored hydrogel matrix would be subjected to massive change which is considered as signal afterwards. The signals are generated by the phase transition of the hydrogel (gel to sol), quenching of the fluorophores used in preparing the matrix, swelling of the matrix, changing the color of the matrix, and disintrigrating the matrix.

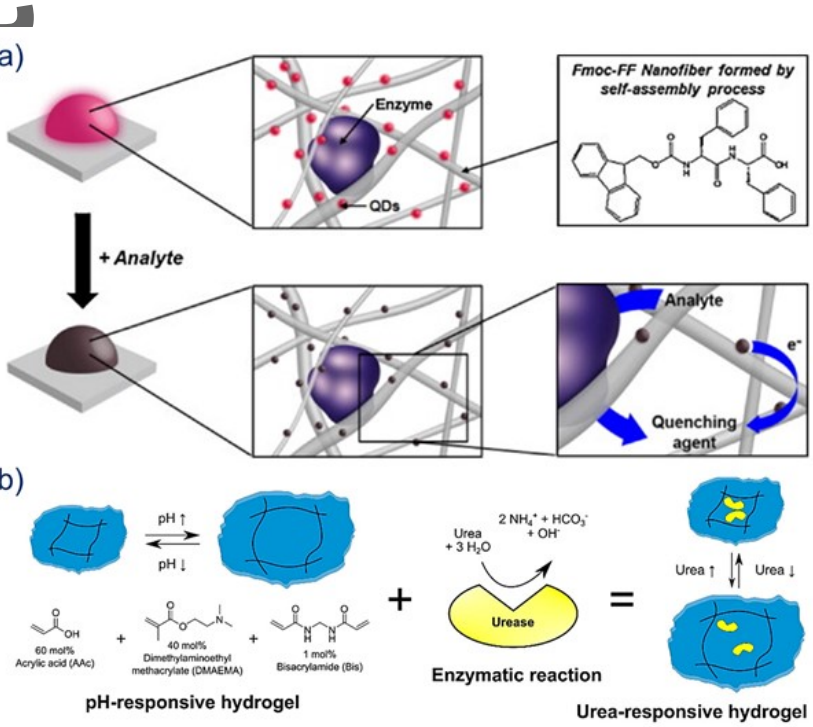

Figure 5. (a) Mechanism of Fmoc-FF hydrogel luminescence quenching. Reproduced with permission.[188] Copyright 2011, Elsevier. (b) Mechanism of pH-sensitive hydrogel system, encapsulant = urease, analyte = urea, sensor = piezoresistive pressure sensor. Reproduced with permission.[192] Copyright 2019, MDPI.

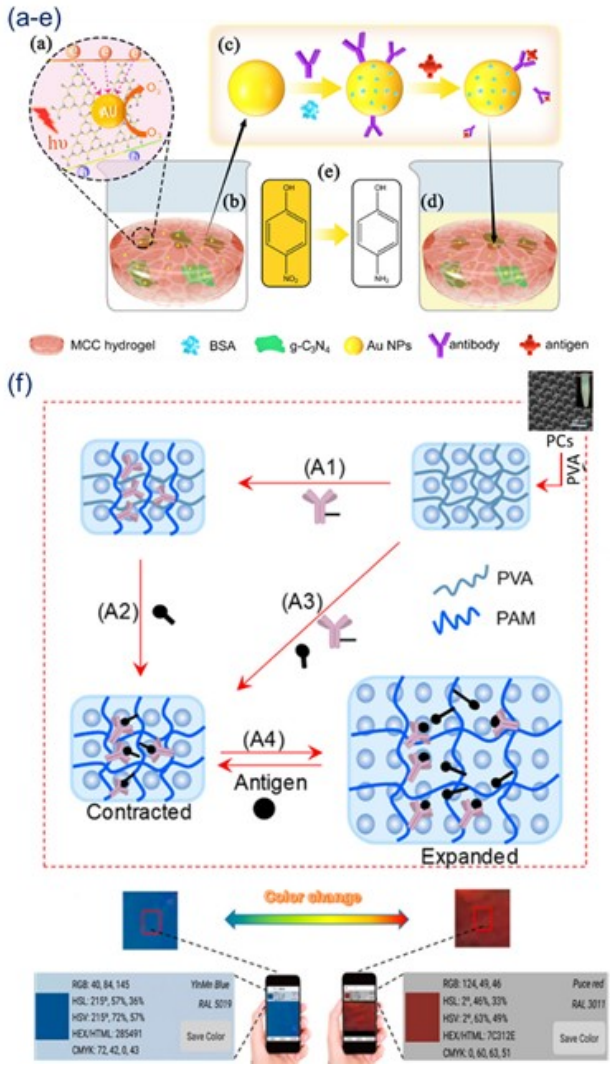

Figure 6. (a-e) Schematic illustration of the colorimetric immunoassay for the detection of α-fetoprotein (AFP) antigen based on the catalytic performance of Au@g-C_3N_4/MCC[a]. (a) Mechanism of the electron transfer between g-C_3N_4 and Au NPs. (b) Color of 4-nitrophenol faded almost completely at the 40th minute catalyzed by Au@g-C_3N_4/MCC. (c) Incubation process of antibody/antigen with Au@g-C_3N_4/MCC. (d) Color of 4-nitrophenol partially faded at the 40th minute catalyzed by incubated Au@g-C_3N_4/MCC. (e) Color and structure of 4-nitrophenol (yellow) and 4-AP (colorless). Reproduced with permission.[201] Copyright 2019, American Chemical Society. (f) Fabrication and workflow of competition-based universal PCH biosensors by using antibody-antigen interaction (A1, A2) Two-step and (A3) single-step polymerization processes in the fabrication of PCH biosensors, which were subsequently used in (A4) for reversible analyte sensing. (B1) Fabrication of conventional PCH biosensors based on the direct method, followed by (B2) analyte

sensing. (inset) SEM image of CPCs, prepared from monodisperse polystyrene nanoparticles (diameter: ~100 nm). (C) Scheme showing the expected color changes in PCH biosensors upon reversible analyte binding, which could be readily detected by either naked eyes or, more quantitatively, a smartphone with an app. (D, E) Schemes showing acrylation of antibodies-antigens used in the current study and the two-step DEAP-initiated polymerization in PCH fabrication. Reproduced with permission.[208] Copyright 2020, American Chemical Society.

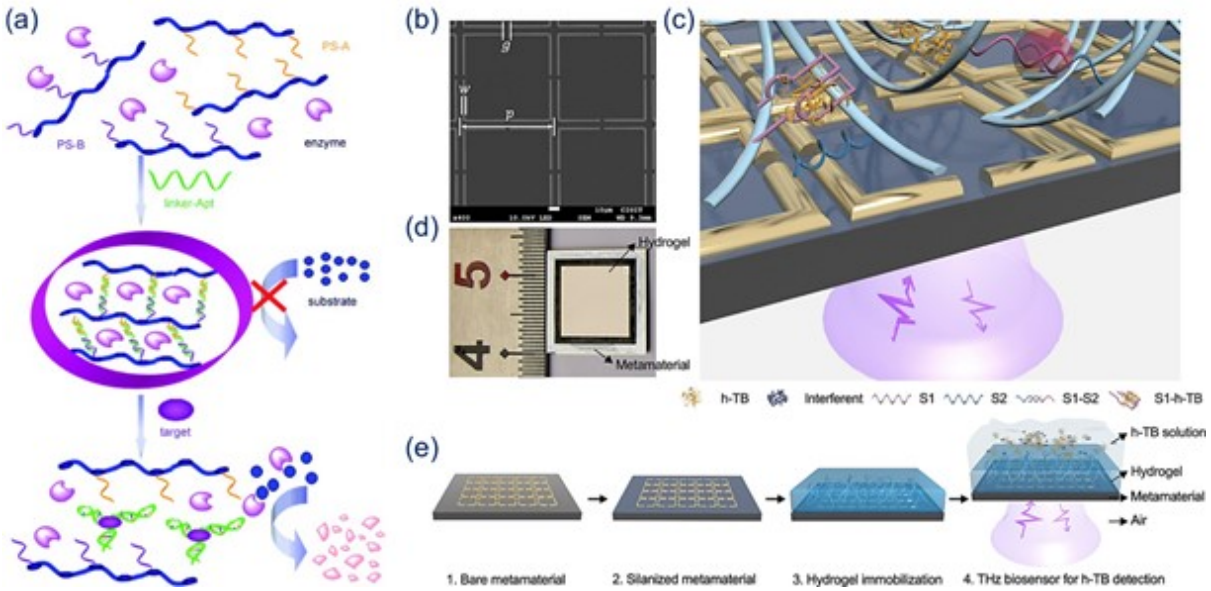

Figure 7. (a) Aptamer-target binding resulting gel disassembly. Reproduced with permission.[211] Copyright 2010, Wiley-VCH. (b) SEM image of the bare THz metamaterial. (c) Schematic representation of h-TB sensing by the THz biosensor. (d) The physical image of the THz biosensor. (e) Experimental procedure of the proposed strategy. Reproduced with permission.[223] Copyright 2021, American Chemical Society.

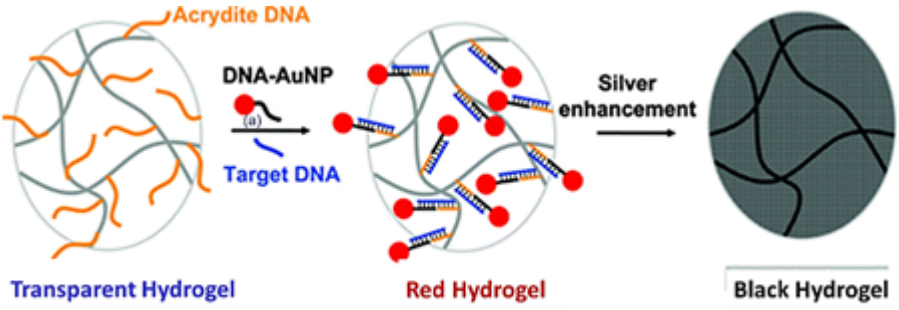

Figure 8. The use of DNA-functionalized hydrogels and AuNPs for colorimetric DNA detection. When the target DNA is present, the color of the transparent gels changes to red. Signal amplification can be accomplished by lowering Ag^+ in the presence of AuNPs to coat the gel with metallic silver. Reproduced with permission.[129] Copyright 2010, American Chemical Society.

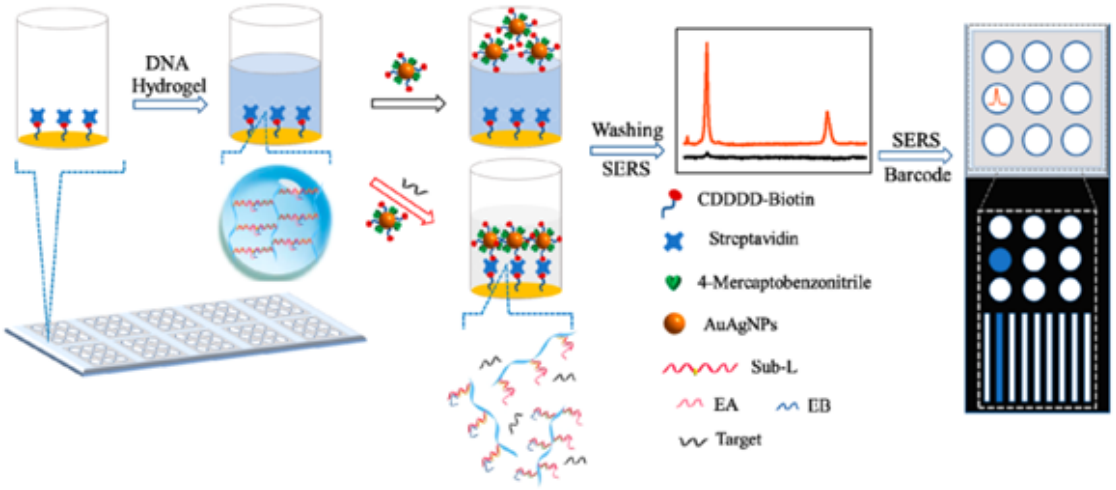

Figure 9. Schematic representation of the preparation of the target miRNA-responsive DNA hydrogel and design of AuAgNPs tagged SERS array sensor for multiple measurements of single sample in one chip. Reproduced with permission.[236] Copyright 2020, American Chemical Society.

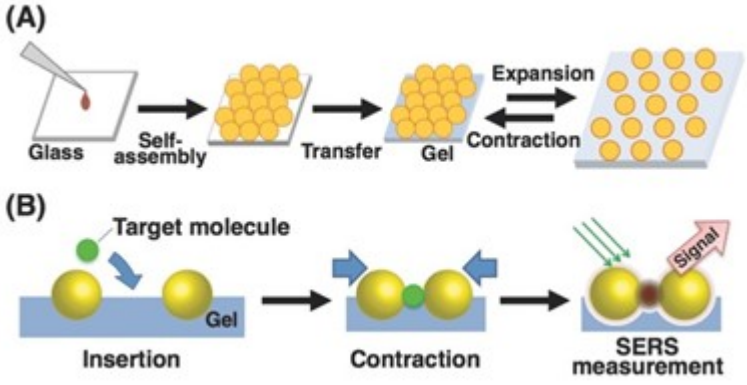

Figure 10. Schematic representation of the design of tunable plasmonic AuNPs and their application for SERS detection of protein. Reproduced with permission.[246] Copyright 2015, WILEY-VCH.

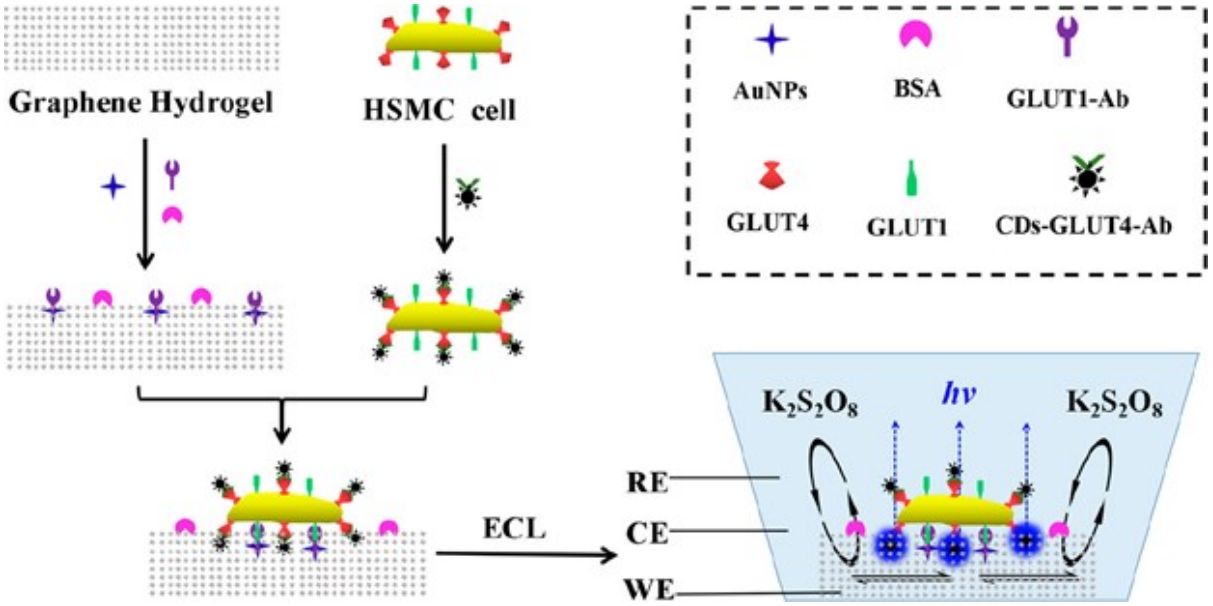

Figure. 11. Fabrication of graphene hydrogel-functionalized ECL cytosensor for quantitative detection of glucose transporter 4 expressions at skeletal muscle cells. Reproduced with permission.[255] Copyright 2019, American Chemical Society.

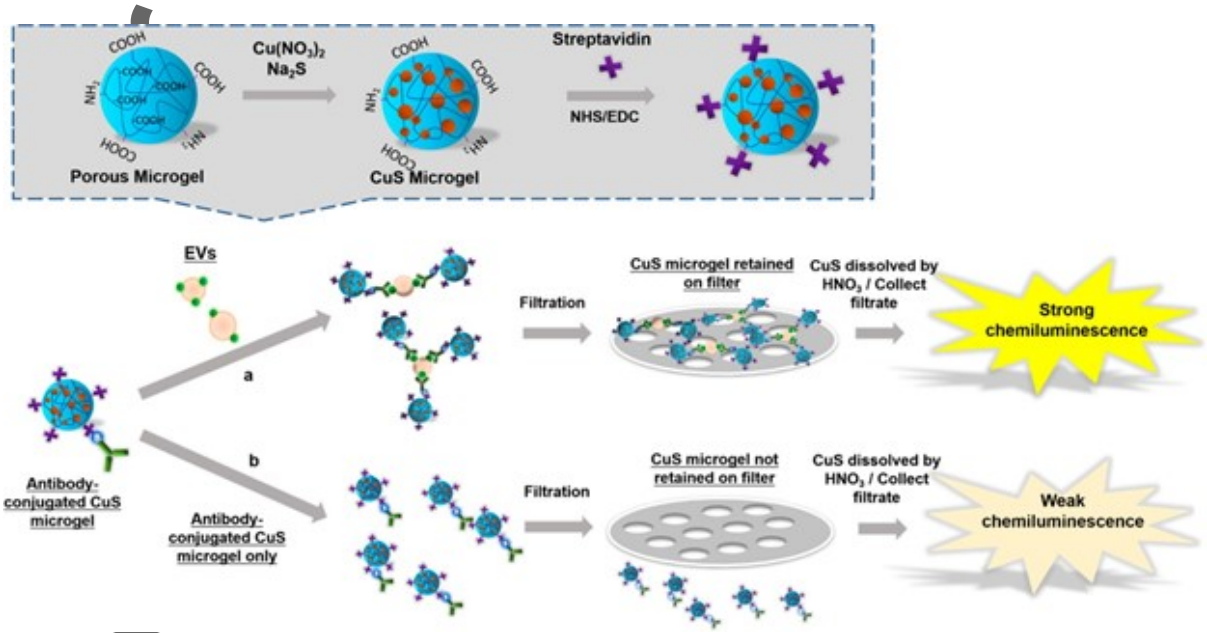

Figure 12. Schematic illustration of hydrogel microparticles (CuS-MG) Synthesis (grey part) and the CuS-MG-based isolation and ECL quantification of EV (lower part). Reproduced with permission.[263] Copyright 2019, American Chemical Society.

Table 1 Hydrogel nanostructure based biosensors for disease-specific biomarkers (*e.g.*, nucleic acids,

Biomarkers		Hydrogel composition	Nanostructure	Signal Readout	Recognizer	Linear range	LOD	Ref.
DNA	Circulating tumor DNA (ctDNA)	DNAzyme hydrogel	None	Colorimetric Assay	G-quadruplex/hemin complex	1 pM -10 nM	0.32 pM	[264]
	Alzheimer biomarker (tDNA)	Alkaline phosphatase@DNA hydrogel	AuNPs	Cyclic voltammetry	Redox reaction catalyzed by ALP	1×10^{-2} - 1×10^{4} pM	3.4×10^{-3} pM	[265]
RNA	miRNA-24	PAni/phytic acid hydrogel	None	Differential pulse voltammetry	DNA probe	1.0 fM-1.0 pM	0.34 fM	[266]
	miRNAs	DNA hydrogel	AuAgNPs	SERS	DNA probe	Not reported	Not reported	[267]
	miRna-21	Carbon dot/Chitosan	Carbon dots	Fluorescence Quenching spectra	DNA probe	0.1-125 fM	0.03 fM	[268]
	miRNA (has-led-7d-5p)	DNA hydrogel	AuNPs	Cyclic Voltammetry	Oligo probe	1 fM- 10 pM	0.35 fM	[269]
	multiplexed miRNA	Poly(ethylene) glycol diacrylate (PEGDA) hydrogel	None	Fluorescence spectra	ssDNA probe	Not reported	2.5 amol	[270]
Protein	Thrombin	PVA-borax hydrogel (PBH)	AuNPs	Resonance Rayleigh Scattering	Thiolated-TBA	0.70 pM – 0.02 μM	0.10 pM	[271]
	Cardiac troponin 1(cTn 1)	PEGDA-gelatin	Photonic Crystals	Fluorescence Spectra	cTn 1 antibody	0.01-1000 ng/mL	0.009 ng/mL	[272]
	B-type natriuretic peptide (BNP)	PEGDA-gelatin	Photonic crystals	Fluorescence Spectra	BNP antibody	0.1-10000 pg/mL	0.084 pg/mL	[272]
	Myoglobin	PEGDA-gelatin	Photonic crystals	Fluorescence Spectra	Myo antibody	1-10000 ng/mL	0.68 ng/mL	[272]
Circulating tumor/cancer cell	MCF-7 cell	3D DNA hydrogel	None	Confocal microscopic imaging	Aptamer toehold biblocks	Not reported	10 cells in 2 μL blood	[273]
Exosomes	Prostate cancer specific exosome	DNA hydrogel	AuNPs	Surface plasmon resonance imaging (SPRi)	Aptamer	1×10^{5} - 1×10^{7} particles/mL	1×10^{5} particles/mL	[274]

proteins, antibodies, extracellular vesicles, exosomes, circulating tumor cell.

Authors Biography

Zakia Sultana Nishat is a graduate student at Shahjalal University of Science and Technology's School of Life Science, where she is pursuing a master's degree in Biochemistry and Molecular Biology. Besides academic coursework, she has been actively engaged in research arena including computational chemistry, biomolecular simulation, and bioinformatics. Her interests span structural biology, quantum chemistry, and nanomaterial science. She wants to converge nano scale, atomic scale, and quantum scale to explore the behavior of biomolecules.

Prof. Yusuke Yamauchi received his Ph.D. degree in 2007 from Waseda University, Japan. After that, he joined NIMS to start his own group. In 2017, he joined the University of Queensland (UQ), Australia as a full-time professor. He concurrently serves as an honorary group leader in NIMS and associate editor of the Journal of Materials Chemistry A and the Chemical Engineering Journal. His expertise is on the fabrication of nanoporous materials via materials architectonics for energy storage and conversion applications.

Dr. Mostafa Kamal Masud obtained his PhD from UQ, Australia in 2020. He received his MS and B.Sc. (Hons.) in Chemistry from Shahjalal University of Science and Technology, Bangladesh. Currently, he is working as a JSPS Postdoctoral Fellow at National Institute for Materials Science (NIMS), Japan. He concurrently serves as an Honorary Fellow at Australian Institute for Bioengineering and Nanotechnology (AIBN), UQ, Australia. His research focuses on the design and translation of bio-favorable engineered nanostructured superparamagnetic materials towards the development of molecular diagnostics (optical and electrochemical nanobiosensors, magnetophoretic and paper-based biosensors) to address critical issues in medical diagnosis.

WILEY-VCH

TOC

Hydrogel nanoarchitectonics: an evolving paradigm for ultrasensitive biosensing

Zakia Sultana Nishat, Tanvir Hossain, Md. Nazmul Islam, Hoang-Phuong Phan, Md A. Wahab, Mohammad Ali Moni, Carlos Salomon, Mohammed A. Amin, Abu Ali Ibn Sina, Md Shahriar A. Hossain, Yusuf Valentino Kaneti,* Yusuke Yamauchi, Mostafa Kamal Masud*

Hydrogel nanoarchitectonics provide the opportunities to design physically- and chemically-controlled and optimized soft structures with synergistic properties and unique nanostructures for promoting responsiveness to mechanical, optical, thermal, magnetic, and electrical stimuli, which in turn open avenues for fabricating next-generation robust biosensors for clinical settings.